ORNL/TM-2020/1500/v3

SCALE 6.2.4 Validation: Reactor Physics

Germina Ilas
Joseph R. Burns
Briana D. Hiscox
Ugur Mertyurek

November 2022

OAK RIDGE National Laboratory

ORNL IS MANAGED BY UT-BATTELLE LLC FOR THE US DEPARTMENT OF ENERGY

ORNL/TM-2020/1500/v3

Nuclear Energy and Fuel Cycle Division

SCALE 6.2.4 VALIDATION: REACTOR PHYSICS

Germina Ilas
Joseph R. Burns
Briana D. Hiscox
Ugur Mertyurek

Date Published: November 2022

Prepared by
OAK RIDGE NATIONAL LABORATORY
Oak Ridge, TN 37831-6283
managed by
UT-BATTELLE, LLC
for the
US DEPARTMENT OF ENERGY
under contract DE-AC05-00OR22725

CONTENTS

LIST OF FIGURES

LIST OF TABLES

ABBREVIATIONS

2D	two-dimensional
3D	three-dimensional
BC	burnup credit
BI	burnup indicator
ANL	Argonne National Laboratory
ATM	approved testing material
BWR	boiling water reactor
CE	continuous energy
C/E	calculated-to-experimental ratio
CEA	Commissariat à l'Énergie Atomique
CR	[NRC] contractor report
DOE	US Department of Energy
ENDF	Evaluated Nuclear Data File
GE-VNC	General Electric Vallecitos Nuclear Center
HTGR	high-temperature gas-cooled reactor
HTR	High-Temperature Reactor
HTTR	High-Temperature Test Reactor
IAEA	International Atomic Energy Agency
ICPMS	inductively coupled plasma mass spectrometry
ID	isotope dilution
IRCh	Institute for Radiochemistry at Karlsruhe
ITU	European Institute for Transuranium Elements
JAERI	Japan Atomic Energy Research Institute (now Japan Atomic Energy Agency)
JRC	Joint Research Center, European Commission
KRI	Khlopin Radium Institute
LWR	light water reactor
MC-ICPMS	multi-collector inductively coupled plasma mass spectrometry
MG	multigroup
MOC	method of characteristics
MOX	mixed oxide
NE	[DOE] Office of Nuclear Energy
NEA	Nuclear Energy Agency
NNSA	National Nuclear Energy Administration
NRC	US Nuclear Regulatory Commission
NUREG	[NRC] nuclear regulatory report
ORNL	Oak Ridge National Laboratory
PNL	Pacific Northwest National Laboratory
PSI	Paul Scherrer Institute
PWR	pressurized water reactor
RCA	radiochemical assay
RS	radiation shielding
SCK·CEN	Studiecentrum voor Kernenergie – Centre d'étude de l'Énergie Nucléaire
SFWST	Spent Fuel and Waste Science and Technology
TIMS	thermal ionization mass spectrometry
TMI	Three-Mile Island
TRISO	tristructural isotropic
WBN1	Watts Bar Nuclear Unit 1
WAK	Karlsruhe Reprocessing Plant
WM	waste management
YMP	Yucca Mountain Project

ACKNOWLEDGMENTS

Funding for this work was provided by the US Nuclear Regulatory Commission. This validation study is a continuation of previous validation research and has benefitted from all related efforts over the past few decades of SCALE's history. The contributions of all who directly participated to the preceding experimental data collection and evaluation, modeling and simulation of experiments, and documentation of investigations are much appreciated and acknowledged. This previous research provided a solid basis for our current and future assessments.

ABSTRACT

This report is the third volume in a report series documenting the validation of SCALE 6.2.4, which is used herein with ENDF/B-VII.1 libraries, for nuclear criticality safety, reactor physics, and radiation shielding applications. This report focuses on validating SCALE capabilities that affect reactor physics applications. The experimental data used as basis for validation consists of measurement data for nuclide inventory, decay heat, and full-core experiments and include the following:

1. radiochemical assay measurements of 40 nuclides of importance to burnup credit, decay heat, and radiation shielding in 169 light-water reactor (LWR) spent nuclear fuel samples that cover burnups up to 70 GWd/MTU and initial enrichments up to 4.9% ^{235}U;

2. full-assembly decay heat measurements for 236 LWR assemblies with

    a. initial fuel enrichments up to 4% ^{235}U,

    b. assembly burnups of 5–51 GWd/MTU, and

    c. cooling times after discharge in the 2- to 27-year range (of importance to spent nuclear fuel storage, transportation, and disposal); and

3. pulse fission irradiations for fissionable materials at cooling times of interest to severe accident analyses ($<10^5$ s).

Validation examples for full-core analysis are based on startup experiments for the Watts Bar Nuclear Unit 1 (WBN1) pressurized water reactor (PWR) and two high-temperature gas-cooled reactor (HTGR) benchmarks for the HTR-10 pebble bed and the prismatic HTTR reactor.

The results for nuclide inventories show improved prediction when compared to those from corresponding analyses performed with SCALE 6.1 and ENDF/B-VII.0 libraries. These improvements were seen in a series of actinides and fission products, particularly plutonium isotopes. The calculated-to-experimental (C/E) ratio for the major actinide ^{239}Pu is 1.019 (σ=0.034) for PWR measurements and 0.974 (σ=0.085) for boiling water reactor (BWR) measurements. A good agreement is obtained between calculated and experimental assembly decay heat, with an average C/E over all considered measurements of 1.006 (σ=0.016) for PWR experiments and 0.984 (σ=0.077) for BWR experiments. The full-core validation for WBN1 shows a calculated eigenvalue consistent with the experiment (10 pcm difference) and a predicted differential boron worth within 5% of the measurement. The calculated eigenvalue for the HTR-10 benchmark agrees well with the experiment, being approximately within the reported experimental uncertainty of 370 pcm. For the HTTR benchmark, the calculation overestimates the experiment by ~500 pcm.

Quantifying and understanding the bias in predicting key metrics such as nuclide inventories and decay heat is essential for evaluating the performance of fuel depletion capabilities and associated nuclear data in SCALE 6.2.4. The impact of the validation findings goes well beyond spent nuclear fuel transportation and storage applications to support modeling challenges in other areas, such as isotope production, national security, and nonproliferation applications. Adequately simulating nuclide transmutations and decay in nuclear fuel during and post irradiation is of great importance in these areas.

1. INTRODUCTION

This report is the third volume in a report series documenting the validation of SCALE 6.2.4 [1], which is used with Evaluated Nuclear Data File (ENDF)/B-VII.1 nuclear data [2] libraries, for nuclear criticality safety, reactor physics, and radiation shielding applications. This report focuses on validating SCALE capabilities that affect reactor physics applications. This validation is based on measurement data from nuclide inventory, decay heat, and full-core experiments.

The nuclide inventory experimental data include radiochemical assay (RCA) measurements for 40 nuclides of importance to burnup credit, decay heat, and radiation shielding in (a) 92 pressurized water reactor (PWR) spent nuclear fuel samples with burnups 7-70 GWd/MTU and initial enrichments 2.4–4.7% ^{235}U, and (b) 77 boiling water reactor (BWR) spent nuclear fuel samples covering 4.2 to 68.4 GWd/MTU burnups, 2.1 to 4.94% ^{235}U initial enrichments, and 0–74% average void fraction during irradiation at the sample location. Twenty-six of the BWR samples were selected from UO_2-Gd_2O_3 fuel rods with 3.0 to 5.0% Gd_2O_3 loading.

The decay heat validation basis includes (a) full-assembly decay heat measurements for light-water reactors (LWRs) at cooling times after discharge of importance to spent nuclear fuel storage, transportation, and disposal, and (b) pulse fission irradiations for fissionable materials for cooling times of interest to severe accident analyses ($< 10^5$ s). There are 91 PWR full assembly decay heat measurements considered, covering a burnup range of 18–51 GWd/MTU, a cooling time between 4.5 and 27.7 years, and an initial fuel enrichment from 2.1 to 4.0% ^{235}U. The BWR decay heat measurement data include 145 measurements covering assembly burnups of 5–45 GWd/MTU, a cooling time range of 2.3–26.7 years, and initial assembly-average fuel enrichments of 1.1 to 2.9% ^{235}U.

Validation examples for full-core analyses are based on startup experiments for the Watts Bar Nuclear Unit 1 (WBN1) PWR and two high-temperature gas cooled reactors (HTGRs): the HTR-10 pebble bed reactor and the prismatic high-temperature test reactor (HTTR). Although SCALE does not have a core simulator to model the operation history of very large configurations such as an LWR, it could serve and has been used for providing continuous-energy (CE) reference solutions for verification of multigroup (MG) analyses performed with LWR core simulators. Ongoing efforts at Oak Ridge National Laboratory (ORNL) for modeling and evaluating with SCALE several advanced non-LWR reactor systems to quantify source terms for severe accidents are documented in the literature. Once the associated full-core models are finalized and documented, they will become part of the SCALE validation basis in future validation reports. In this report, only non-LWR models that were documented by the time of this writing are included.

The validation documented herein is not exhaustive, although it includes a large number of relevant validation cases for the considered nuclide inventory and decay heat metrics. Validation for neutron and gamma spectra in spent nuclear fuel, which is of particular interest to nuclear safeguards and nonproliferation applications, is not addressed in this report. However, such validation studies are available in the literature [3–5].

A brief review of previous ORNL efforts on SCALE validation for reactor physics applications is provided in Section 2. Sections 3 through 5 present the validation results for nuclide inventory, decay heat, and full-core analysis. Each of these sections discusses the experimental data used as a validation basis, the computational models used, and the comparison of calculation to experiment. Comparisons of results obtained with SCALE 6.2.4/ENDF/B-VII.1 and corresponding available results calculated with SCALE 6.1/ENDF/B-VII.0 are also included. The summary and concluding remarks are presented in Section 6.

2. BRIEF REVIEW OF PREVIOUS SCALE VALIDATION FOR REACTOR PHYSICS APPLICATIONS

Validation of capabilities and associated nuclear data in the SCALE code system to support reactor physics applications has been a continuous effort at ORNL since these capabilities were first developed. Before the 2000s, when lattice physics or full-core capabilities for complex configurations were still only in the research phase, validation analyses focused on source terms for spent nuclear fuel. For example, SCALE-4.2 with ENDF/B-V nuclear data were used to validate nuclide predictions in spent nuclear fuel based on experimental assay data for 38 fuel samples irradiated in five PWRs operated in Germany, Italy, and the United States: Calvert Cliffs 1, H.B. Robinson 2, Obrigheim, Trino Vercellese, and Turkey Point 3 reactors [6, 7]. The large majority of these samples had burnups lower than 35 GWd/MTU, and the measurements included mostly actinides. Under a project sponsored by the US Nuclear Regulatory Commission (NRC) that was initiated in the 2000s, ORNL acquired new experimental assay data representative of more modern fuel designs and higher burnups. These data were acquired through domestic and international experimental programs. These newly collected experimental data, which were used along with other available measurements to validate depletion capabilities in SCALE 5.1, included samples selected from fuel irradiated in the GKN II, Gosgen, Takahama 3, Three-Mile Island (TMI)-1 and Vandellos II reactors, and they are documented in a series of NRC nuclear regulatory (NUREG) / contractor reports (CRs) [8-11] focused on high-burnup fuels.

Since 2010, efforts have been focused on compiling new and old experimental assay data for 118 PWR fuel samples [12] to cover both low and high burnup ranges. These 118 samples originated from fuel irradiated in the Calvert Cliffs 1, GKN II, Gosgen, H.B. Robinson 2, Obrigheim, Takahama 3, TMI-1, Trino Vercellese, and Turkey Point 3 reactors. The measurements for these 118 samples were documented and used with SCALE 5.1 and ENDF/B-V cross section data to determine C/E nuclide concentration ratios for the measured nuclides [12]. The 118 PWR sample data also served as the basis for the PWR isotopic validation to support burnup credit in NUREG/CR-7108 [13, 14]. The calculations at that time were performed with SCALE 6.1 [15] and ENDF/B-VII.0 [16] libraries. Since circa 2010, ORNL measured and analyzed six new PWR samples under support of the US Department of Energy (DOE) / Office of Nuclear Energy (NE) and the National Nuclear Energy Administration (NNSA). Of the six samples, one was from Calvert Cliffs 1 fuel [17], and five samples were from TMI-1 fuel [18]. These were modeled with SCALE 6.1 and ENDF/B-VII.0 data. The same set of 92 PWR measurement data used as the validation basis in the current report was previously used to validate depletion capabilities in SCALE 6.1/ENDF/B-VII.0 [19].

Validation of SCALE 4.3 with ENDF/B-V data for nuclide inventories in BWR spent fuel were documented in 1998 [20] for 30 measured samples from fuel irradiated in the Cooper reactor (US), the Gundremmingen reactor (Germany), and the Japan Power Demonstration Reactor (JPDR). In 2010, 32 BWR measured samples from fuel irradiated in Fukushima Daini 2 (Japan), Cooper, and Gundremmingen reactors served to validate SCALE 5.1 used with ENDF/B-V data [21]. Under a BWR burnup credit study funded by NRC in the 2010s, an expanded validation basis for BWR nuclide inventory was identified. This basis was documented in 2016 [22, 23] and included 77 samples from fuel irradiated in Dodewaard (Belgium), Fukushima Daini 1 and 2, Forsmark 3 (Sweden), Leibstadt (Switzerland), and Limerick (US) reactors.

As part of an effort to develop ORIGEN reactor libraries for mixed oxide (MOX) fuel, validation for MOX nuclide inventories (not covered in the current report) was performed with SCALE 6.1/ENDF/B-VII.0 and was based on PWR and BWR MOX fuel measured under the MALIBU international experimental program [24]. Additionally, measurements for one of these MOX samples, along with a PWR sample and a BWR sample, were used for a recent lattice physics assessment [25] of the new Polaris LWR lattice physics code [26] introduced in SCALE 6.2.

Validation for pulse fission experiments with SCALE 5.1/ENDF/B-V was documented in 2006 [27]. A comprehensive decay heat validation was first documented for SCALE 5.1/ENDF/B-V [28] and included full-assembly decay heat and pulse fission experimental data as the validation basis. Subsets of these experimental data were the object of detailed analysis with SCALE 5.1/ENDF/B-V [29] and SCALE 6.1/ENDF/B-VII.0 [30], along with analysis of uncertainty in calculated decay heat that resulted from modeling data uncertainties [31].

An extensive SCALE validation for modeling HTGRs, carried out during the 2010s, included validation for full-core HTGRs models of HTR-10, HTTR, and PROTEUS pebble bed configurations [32–34]. The simulations were performed with SCALE 6.1 and ENDF/B-VII.0 cross sections. Recently, the HTR-10 and HTTR were also included in an assessment of SCALE's capabilities for HTGR analysis [35]. The largest full-core model ever developed with SCALE was for the WBN1 PWR [36, 37], with the purpose of providing a CE reference solution to verify MG calculations with the VERA core simulator [36]. This model for the WBN1 initial critical configuration included nine million lines of ASCII input containing 800,000 unique geometry units. The model required 100 billion particle histories to produce a reliable reference for a three-dimensional (3D) pin-by-pin power distribution.

The validation studies mentioned in this section are only selected examples of numerous ORNL validation efforts; moreover, the studies discussed here do not encompass the multitude of previous validation publications authored by non-ORNL researchers.

3. NUCLIDE INVENTORY

This section presents comparisons of calculated nuclide contents in PWR and BWR spent nuclear fuel to RCA measurements for these nuclides. To facilitate understanding of the bias's potential impact on calculated nuclide contents, the relative importance of most measured nuclides to key metrics characterizing spent nuclear fuel is summarized first.

3.1 NUCLIDE IMPORTANCE TO SAFETY APPLICATIONS

High-quality RCA data for spent nuclear fuel are essential for evaluating uncertainties in spent nuclear fuel safety analyses, including burnup credit, decay heat, neutron and gamma sources, or waste management applications. In particular, these data provide one means for determining uncertainties in integral quantities important to safety, such as decay heat or spent fuel reactivity. Direct measurements of such integral quantities can be expensive or impractical for the multitude of existing fuel designs, operating conditions, and specific application purposes. However, as these integral quantities are mainly driven by the nuclide composition in spent fuel at the end of irradiation and the cooling time after discharge, measured nuclide compositions can serve as an indirect way to determine the uncertainties associated with code predictions of these integral quantities.

Previous studies have investigated nuclides of high relevance to various reactor safety applications and the relative importance of these nuclides to the metrics characterizing spent nuclear fuel [38-40]. Findings from these investigations are summarized herein.

Table 1 presents a list of 58 nuclides [40] that are highly important to burnup credit in criticality safety analysis, radiological safety, and waste management applications and for which RCA data are generally available.

3.1.1 Nuclides Important to Burnup Credit

Burnup credit is a term commonly used in criticality safety analyses and refers to taking credit of reactivity changes in systems containing spent nuclear fuel that are due to fuel burnup. Table 2 lists 28 nuclides that are of high importance to burnup credit for storage and transportation of spent nuclear fuel discharged from commercial power reactors [13]. These nuclides consist of 12 actinides and 16 fission products with large neutron fission cross sections and/or large neutron absorption cross sections. The relative importance of these nuclides to spent fuel reactivity varies with burnup, cooling time, initial fuel enrichment, and assembly design. Nine of the 12 actinides listed in Table 2 (^{234}U, ^{235}U, ^{238}U, ^{238}Pu, ^{239}Pu, ^{240}Pu, ^{241}Pu, ^{242}Pu, and ^{241}Am) account for ~ 95% of the reactivity's worth of the actinides and ~70% of the total reactivity's worth of all nuclides in typical spent fuel, whereas 6 of the listed 16 fission products (^{143}Nd, ^{149}Sm, ^{103}Rh, ^{151}Sm, ^{133}Cs, and ^{155}Gd) account for ~75% of the fission product reactivity's worth and ~20% of the total reactivity's worth in typical spent fuel [39].

Table 1. Nuclides important to spent fuel safety applications [40].

Nuclide	Half life	Burnup credit	Radiological safety	Waste management
^{79}Se	2.95×10^5 years			■
^{95}Mo	Stable	■		
^{90}Sr/^{90}Y	28.9 years		■	■
^{99}Tc	2.11×10^5 years	■		■
^{101}Ru	Stable	■		
^{106}Ru	371.6 days		■	
^{103}Rh	Stable	■		
^{109}Ag	Stable	■		
^{125}Sb	2.76 years		■	
^{129}I	1.6×10^7 years			■
^{133}Cs	Stable	■		
^{134}Cs	2.06 years		■	
^{135}Cs	2.3×10^6 years			■
^{137}Cs/^{137}Ba	30.0 years		■	■
^{139}La[a]	Stable			
^{143}Nd	Stable	■		
^{145}Nd	Stable	■		
^{148}Nd[a]	Stable			
^{144}Ce/^{144}Pr[a]	284.9 days		■	
^{155}Gd	Stable	■		
^{147}Sm	1.06×10^{11} years	■		
^{149}Sm	Stable	■		
^{150}Sm	Stable	■		
^{151}Sm	90 years	■		
^{152}Sm	Stable	■		
^{151}Eu	Stable	■		
^{153}Eu	Stable	■		
^{154}Eu	8.59 years		■	
^{155}Eu[b]	4.75 years	■	■	
^{234}U	2.45×10^5 years	■		■
^{235}U	7.04×10^8 years	■		■
^{236}U	2.34×10^7 years	■		■
^{238}U	4.47×10^9 years	■		■
^{237}Np	2.14×10^6 years	■		■
^{238}Pu	87.71 years	■	■	■
^{239}Pu	2.41×10^4 years	■	■	■
^{240}Pu	6.56×10^3 years	■	■	■
^{241}Pu	14.29 years	■		■
^{242}Pu	3.75×10^5 years	■		■
^{241}Am	433 years	■	■	■
^{243}Am	7370 years	■		■
^{242}Cm	162.8 days		■	
^{243}Cm[c]	29.1 years	■		
^{244}Cm	18.1 years		■	
^{245}Cm	8.5×10^3 years	■		■
246Cm[c]	18.1 years		■	

[a] Nuclides used as burnup indicators;
[b] Important not directly, but as parent nuclide of ^{155}Gd;
[c] Important for very high burnup.

Table 2. Nuclides important to burnup credit for storage and transportation [13].

^{234}U	^{235}U	^{236}U	^{238}U	^{237}Np	^{238}Pu
^{239}Pu	^{240}Pu	^{241}Pu	^{242}Pu	^{241}Am	^{243}Am
^{95}Mo	^{99}Tc	^{101}Ru	^{103}Rh	^{109}Ag	^{133}Cs
^{143}Nd	^{145}Nd	^{147}Sm	^{149}Sm	^{150}Sm	^{151}Sm
^{152}Sm	^{151}Eu	^{153}Eu	^{155}Gd	–	–

3.1.2 Nuclides Important to Decay Heat

The most important nuclides for decay heat in typical high burnup LWR spent fuel as a function of cooling time are illustrated in Figure 1 [39] for fuel with 4.5% ^{235}U initial enrichment and 50 GWd/MTU burnup. This figure shows the fraction of the total decay heat produced by specific nuclides over a cooling time up to 1,000 years. Figure 2 provides another illustration of decay heat contributors over a shorter cooling time range up to 100 years, with the percentage nuclide contribution to the total decay heat being displayed as a function of cooling time for LWR spent fuel with 2.9% ^{235}U initial enrichment and 37 GWd/MTU burnup [31].

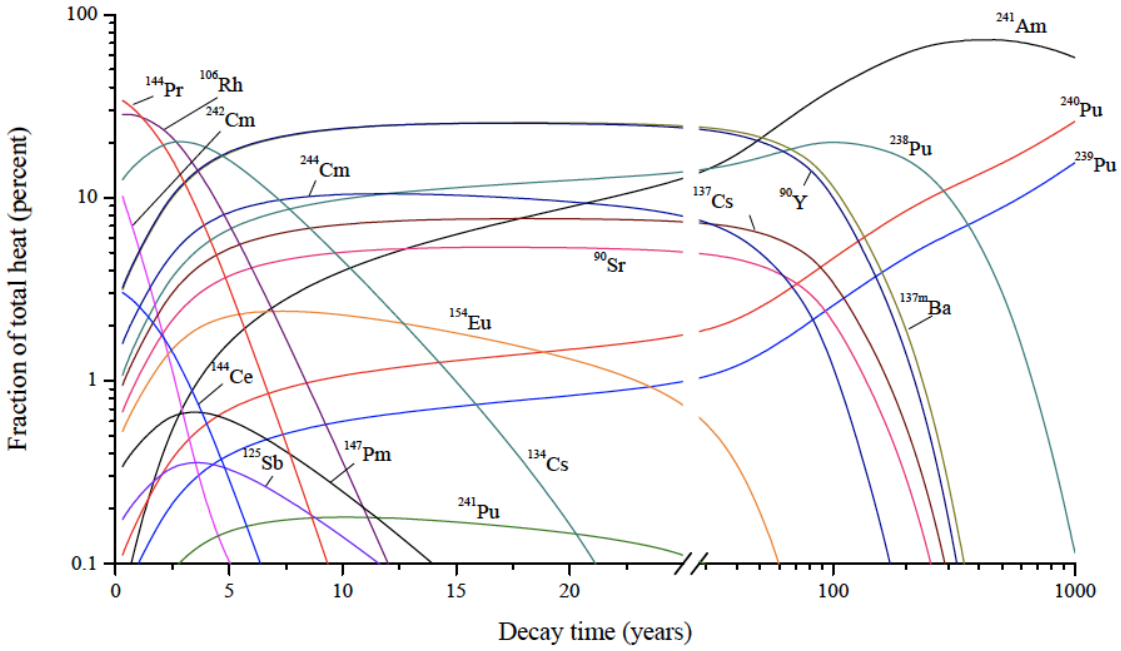

Figure 1. Important nuclides to decay heat for 50 GWd/MTU burnup during 1–1,000 years of cooling time [39].

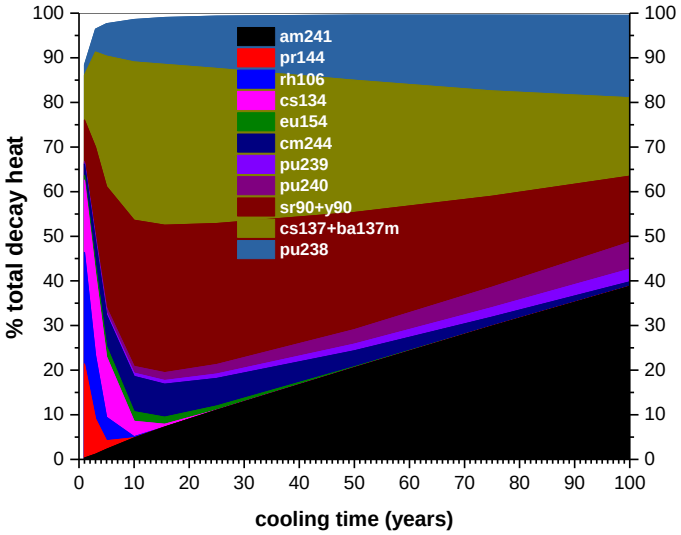

Figure 2. Important nuclides to decay heat for 37 GWd/MTU burnup during 1–100 years of cooling time [31].

At less than 30 days of cooling time, most of major contributors are fission products with short half-lives of minutes or days. The total decay heat decreases in the 30 days after discharge by two orders of magnitude, from ~10^6 W/MTU to ~10^4 W/MTU, while many short-lived fission products decay away. At cooling times from 1 to 50 years, fission products are the main contributors to decay heat, with the top contributors being ^{137}Cs (and its metastable isomer ^{137m}Ba) and ^{90}Sr (and its decay progeny ^{90}Y). The relative contribution to the decay heat of fission products decreases with increasing burnup and increasing cooling time. At cooling times greater than ~50 years, fission products are outranked by ^{241}Am, the concentration of which increases with increasing cooling time due to β-decay of ^{241}Pu (14.4-year half-life). Actinide ^{244}Cm is also a top contributor over a cooling time of approximately 10–100 years. For example, for 50 GWd/MTU fuel, the contribution of ^{244}Cm to decay heat is ~20% at 10 years of cooling time and 15% at 30 years of cooling time. After this point it decreases because this nuclide decays out (18.1-year half-life). At long cooling times over 100 years, ^{241}Am, ^{238}Pu, and ^{239}Pu are the top contributors to decay heat in typical LWR fuel.

3.1.3 Nuclides Important to Shielding

Nuclides of importance to shielding applications are strong neutron and gamma emitters that contribute to dose rates. Many of these nuclides are also important to decay heat. As the spent fuel is generally shielded, the charged particles and low-energy gamma emitters are less important in shielding applications, whereas the nuclides emitting high-energy gammas are major contributors to the gamma dose rates outside the shielded fuel. The nuclide importance varies with the type of shielding material and the shield's thickness.

An assessment of radionuclide importance to the radioactivity of LWR spent fuel and radiation dose rates for three spent fuel casks with different shielding materials (concrete, steel, and lead) showed results [38] for two burnup values—20 and 50 GWd/MTU—and cooling times ranging between 2–10,000 years. The top six nuclides contributing to the total radioactivity of unshielded fuel for the two burnups under consideration at a 5-year cooling time are ^{241}Pu, ^{137}Cs (and progeny ^{137}Ba), ^{90}Sr (and progeny ^{90}Y), and ^{147}Pm. These nuclides contribute more than 10% to the total activity. At a 10,000-year cooling time, a handful of nuclides contribute ~95% to total radioactivity: ^{239}Pu, ^{240}Pu, ^{243}Am, ^{239}Np, and ^{99}Tc.

Another assessment documented by Gauld and Ryman [39] focuses on high burnup fuel, showing nuclide rankings for burnups of 20 and 70 GWd/MTU and 5- and 100-year cooling times. The nuclides contributing more than 1% to the total dose for a steel cask with PWR spent fuel are illustrated in Figure 3. While ^{60}Co, a dominant dose contributor at 5-yr cooling, is produced from activation of the fuel assembly structural materials, the other nuclides shown are present in the spent fuel. For newer assembly designs with new materials having Co at extremely small trace levels compared to the case considered on [39], the impact on dose would be negligible. For the case illustrated in Figure 3, at the 5-year cooling time the fission products contributing with over 10% to the total dose are: ^{144}Pr (progeny of ^{144}Ce) and ^{134}Cs for 20 GWd/t burnup, and ^{134}Cs for 70 GWd/t burnup. The nuclide ^{244}Cm is the only actinide contributing more than 1% to the total dose at this 5-yr cooling time, its contribution increasing significantly with increasing burnup. At the 100-year cooling time, actinides are becoming major contributors, including ^{244}Cm, ^{246}Cm, ^{241}Am, and Pu isotopes; (^{137}Cs-^{137m}Ba) are the only significant fission products contributing with over 1% to total dose at both low and high burnups. At 70 GWd/t burnup, the aggregate contribution to the total dose rate of ^{244}Cm and ^{246}Cm is 70%.

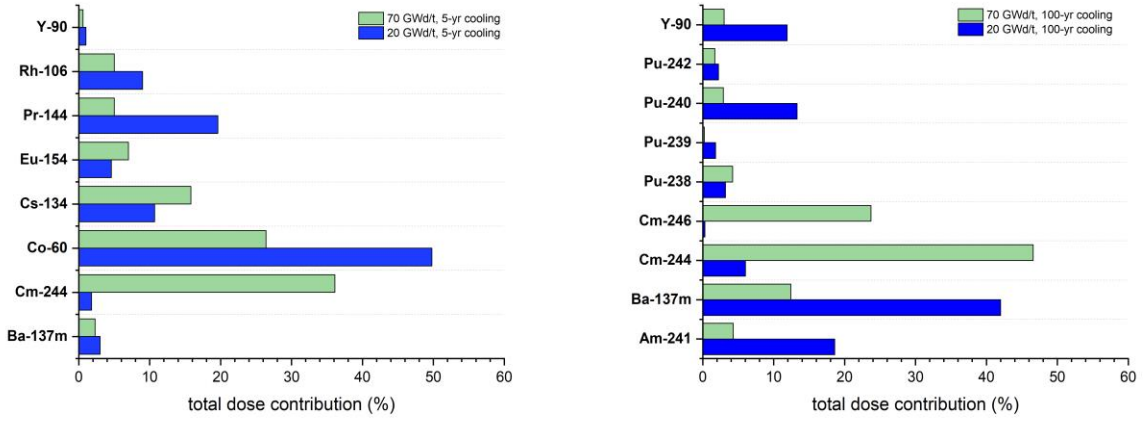

Figure 3. Nuclide contribution to total dose for steel cask (based on data from Gauld and Ryman [39]).

3.2 PWR

3.2.1 Experimental Data

A summary of the PWR RCA data set of 92 spent fuel samples considered in the current validation report is presented in Table 3. This table lists the main characteristics of the fuel rods from which the samples were selected, including assembly lattice, fuel enrichment, and burnup range. These fuel rods were irradiated in nine PWRs that were operated in six countries: Germany, Italy, Japan, Spain, Switzerland, and the United States. The majority of samples were selected from UO_2 fuel rods, with 5 samples selected from UO_2-Gd_2O_3 fuel rods (Takahama fuel).

A large variety of measurement procedures was used at different laboratories and for different experimental programs (Table 3) when performing sampling and dissolution of fuel, isotope separation, mass spectrometry, and radiometric techniques. The type of procedures and techniques are described in detail in the State-of-the-Art Report [40] published by the Nuclear Energy Agency (NEA) in 2011. Radiometric measurements include α-, β-, and γ-spectrometry, or a combination thereof. The minimum percentage of uncertainties associated with these types of measurements is 2–3% at a 95% confidence level; however, the percentage could go up to 10–15%. Thermal ionization mass spectrometry (TIMS) and multi-collector inductively coupled plasma mass spectrometry (MC-ICPMS) are among the most accurate mass spectrometry techniques; they can reach accuracies of 0.1–0.4% when used in tandem with

isotope dilution (ID) as a calibration technique after separation. The main calibration techniques used are (1) isotope dilution, which is based on addition of an element with known isotopic composition, or the "spike," which is added after chemical separation to overcome isobaric interferences, and (2) external calibration, which is based on the use of standards of different concentrations for measurements with no chemical separation. The measurement uncertainties associated with external calibration are typically a few percent.

The reported measurement uncertainties, including their value and significance, differ greatly among measurement laboratories. Across laboratories and different experimental programs [8, 9, 11, 12, 41], there is a general lack of consistency in overall uncertainty vs. spectrometry-only uncertainty. This inconsistency is more prevalent in the experiments performed before modern instruments were available (old vs. new programs). In some cases, the reported experimental uncertainties refer only to instrument precision and are based on multiple measurements of standard solutions. In other cases, the reported uncertainties reflect general laboratory experience in analyzing fuel samples. Recent experimental programs such as ARIANE and MALIBU have reported overall measurement uncertainties for each measured nuclide and sample, including uncertainties resulting from each step involved in the measurement process, beginning with sample cutting and dissolution, all the way through the analysis of the mass spectrometry results [11]. In addition, these programs included analysis of cross-check measurements that were used to confirm estimated measurement uncertainties.

Table 3. Summary of PWR RCA data used for validation.

Reactor	Country	Measurement laboratory [a]	Experimental program	Assembly lattice	Enrichment (% ^{235}U)	No. of samples [c] / fuel rods	Burnup (GWd/MTU)
Calvert Cliffs-1	US	PNL, KRI	ATM-104 [b]	14 × 14	3.038	3/1	27.4–44.3
		PNL	ATM-103	14 × 14	2.72	3/1	18.7–33.2
		PNL, KRI	ATM-106	14 × 14	2.453	3/1	31.4–46.5
GKN II	Germany	SCK·CEN	REBUS [d]	18 × 18	3.8	1/1	54.1
Gösgen	Switzerland	SCK·CEN, ITU	ARIANE [d]	15 × 15	3.5, 4.1	3/2	29.1–59.7
		SCK·CEN, PSI, CEA	MALIBU [d]	15 × 15	4.3	3/1	47.2–70.4
H. B. Robinson-2	US	PNL, LANL	ATM-101	15 × 15	2.561	4/3	16.0–31.7
Obrigheim	Germany	JRC Ispra, Karlsruhe	EUR	14 × 14	2.83, 3.00	15/4	15.6–37.5
		ITU, IRCh, WAK, IAEA	ICE	14 × 14	3.13	5/5	27.0–29.4
Takahama-3	Japan	JAERI	JAERI[f]	17 × 17	2.63, 4.11	13/3	17.4–47.3
TMI-1	US	GE-VNC	DOE YMP[g]	15 × 15	4.657	8/3	22.8–29.9
Trino Vercellese	Italy	JRC Ispra, Karlsruhe	EUR	15 × 15	2.719, 3.13, 3.897	15/5	7.2–17.5
		JRC Ispra, Karlsruhe	EUR	15 × 15	3.13	16/5	12.8–25.3
Turkey Point-3	US	Battelle-Columbus	NWTS	15 × 15	2.556	13/7	19.9–31.6

[a] ANL = Argonne National Laboratory; GE-VNC = General Electric Vallecitos Nuclear Center; PNL = Pacific Northwest National Laboratory; KRI = Khlopin Radium Institute; JAERI = Japan Atomic Energy Research Institute (now Japan Atomic Energy Agency); JRC = Joint Research Center, European Commission; ITU = European Institute for Transuranium Elements; IRCh = Institute for Radiochemistry at Karlsruhe; WAK = Karlsruhe Reprocessing Plant; IAEA = International Atomic Energy Agency; SCK·CEN = Studiecentrum voor Kernenergie – Centre d'étude de l'Énergie Nucléaire; PSI = Paul Scherrer Institute; CEA = Commissariat à l'Énergie Atomique

[b] ATM = approved testing material

[c] Sister samples are not counted here; only the combined data of sister samples are counted, as listed in the reference reports

[d] International Experimental Programs coordinated by Belgonucleaire, Belgium, currently managed by SCK-CEN

[e] One of the three measured rods had UO_2-Gd_2O_3 fuel with 5 measured samples

[f] Two of the three measured rods had UO_2-Gd_2O_3 fuel, for a total of three UO_2-Gd_2O_3 measured samples

[g] DOE YMP = US Department of Energy Yucca Mountain Project

3.2.1.1 Fuel samples characteristics

The distribution of burnup as function of enrichment for the 92 considered samples is illustrated in Figure 4; the colors indicate fuel's origin by reactor name. The histogram of the enrichments and the histogram of the burnups for the considered samples is provided in Figure 5. Almost three quarters of the considered samples originate from fuel of older assembly designs and have enrichments lower than 4.0% ^{235}U. Approximately 87% of the considered samples have burnups lower than 40 GWd/MTU.

Table 4 summarizes the number of measurements available for nuclides that are important for burnup credit, decay heat, and shielding applications, as applicable to the PWR RCA data considered in this validation study. It also shows the ranges of the reported experimental uncertainties for each nuclide, as applicable to the experimental programs under which the measurements were performed. Uranium and plutonium nuclide measurements are available for most of the considered samples.

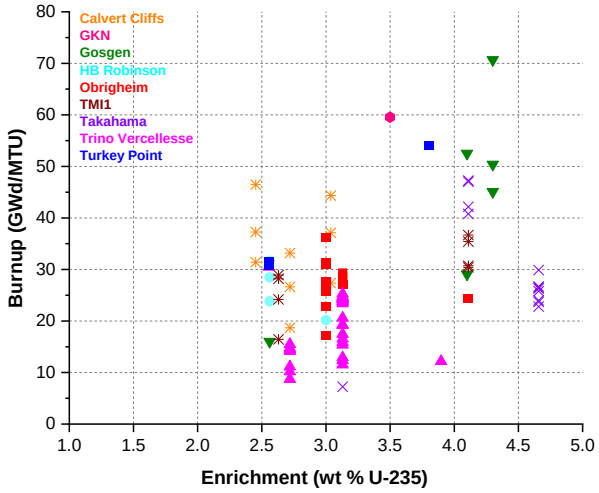

Figure 4. Burnup distribution vs. enrichment for measured PWR samples.

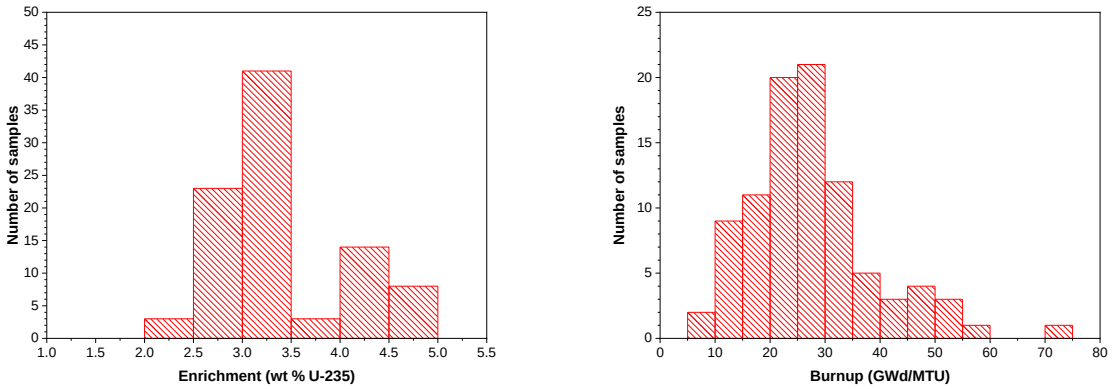

Figure 5. Enrichment and burnup distribution histograms for measured PWR samples.

Table 4. Number of PWR measurements per nuclide.

Nuclide	Number of samples	Application [a]	Reported exp. [b] uncert. (%)
^{234}U	55	BC, WM	0.5 – 5.2
^{235}U	92	BC, WM	0.4 – 3.8
^{236}U	77	BC, WM	0.4 – 2.4
^{238}U	92	BC, WM	0.1 – 4.3
^{238}Pu	77	BC, RS, WM	0.3 – 14.3
^{239}Pu	92	BC, RS, WM	0.3 – 2.4
^{240}Pu	92	BC, RS, WM	0.3 – 2.7
^{241}Pu	92	BC, WM	0.3 – 2.5
^{242}Pu	91	BC, WM	0.3 – 5.3
^{237}Np	36	BC, WM	1.9 – 10.0
^{241}Am	39	BC, RS, WM	1.8 – 20.0
^{243}Am	38	BC, WM	1.8 – 100.0
^{244}Cm	57	RS	0.9 – 28.0
^{245}Cm	24	BC, WM	2.0 – 10.1
^{246}Cm	14	RS	5.0 – 10.1
^{90}Sr	15	RS, WM	1.5 – 8.0
^{99}Tc	20	RS, WM	3.5 – 8.9
^{101}Ru	7	BC	5.0 – 12.2
^{106}Ru	31	RS	3.0 – 12.2
^{103}Rh	8	BC	4.0 – 14.2
^{109}Ag	6	BC	5.0 – 9.1
^{125}Sb	18	RS	5.0 – 9.4
^{133}Cs	10	BC	1.0 – 2.5
^{134}Cs	59	RS	1.5 – 5.0
^{135}Cs	16	WM	1.5 – 14.0
^{137}Cs	73	BI, RS, WM	1.3 – 3.5
^{143}Nd	36	BC	0.1 – 5.1
^{145}Nd	36	BC	0.1 – 5.9
^{148}Nd	77	BI	0.1 – 6.7
^{144}Ce	32	RS	1.7 – 10.0
^{147}Sm	24	BC	0.1 – 10.6
^{149}Sm	20	BC	0.1 – 20.0
^{150}Sm	24	BC	0.1 – 4.2
^{151}Sm	24	BC	0.1 – 38.5
^{152}Sm	24	BC	0.1 – 3.2
^{151}Eu	12	BC	0.9 – 9.8
^{153}Eu	19	BC	0.9 – 5.6
^{154}Eu	44	RS	1.7 – 11.9
^{155}Eu	11	BC	3.2 – 16.1
^{155}Gd	19	BC	1.4 – 6.7

[a] as listed in Table 1; BC=burnup credit, BI=burnup indicator, RS=radiation shielding, WM=waste management

[b] minimum and maximum reported uncertainties for the considered experimental programs

3.2.2 Models

Individual depletion models were developed for each sample, and where data were available, the irradiation history was modeled in detail to include time-dependent values of operating parameters such as soluble boron in coolant, fuel temperature, or coolant density. These models are similar to those applied in previous validation studies [12, 19] that were performed with earlier SCALE versions and different evaluated cross section data. The models are based on the same sources of modeling input data. They are two-dimensional (2D) models, representing quarter, half, or full assembly configurations, depending on the applicable symmetry and the easiness of modeling. The measured fuel rod and the nearest neighboring rods are modeled as unique depletion mixtures (transmutation and decay are tracked separately in these mixtures during the irradiation history simulation), whereas the rest of the UO_2 fuel rods in the assembly are assigned one depletion mixture. For assemblies containing integral burnable absorber rods (UO_2-Gd_2O_3), five to ten rings are defined in these rods, and each ring is mapped with a different depleted mixture to adequately capture the physics behavior of the strong absorber during irradiation.

All PWR depletion simulations were performed with the TRITON [42] 2D depletion sequence in SCALE. In this sequence, TRITON iteratively couples the 2D neutron transport solver NEWT and the ORIGEN nuclear transmutation and decay code [43]. All TRITON simulations were performed using SCALE version 6.2.4 with the 252-group ENDF/B-VII.1 cross section library. For the assemblies that involved changes in the configuration from one irradiation cycle to the other—as was the case for the H.B. Robinson assembly in which absorber rods were removed from the assembly after the first cycle of irradiation—the ***swap*** capability that was newly introduced in SCALE 6.2 was used to easily model configuration changes. Selected depletion models are illustrated in Figure 6 for the Gosgen GU3 sample measured under the ARIANE experimental program and the Calvert Cliffs MKP109-CC sample measured under the ATM-104 experimental program; individual depleted mixtures and other materials are mapped using different colors in these illustrations.

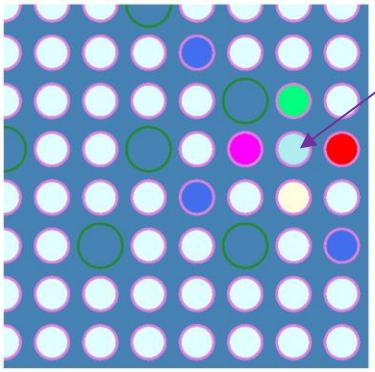

(a) ¼ assembly for Gosgen GU3 sample model

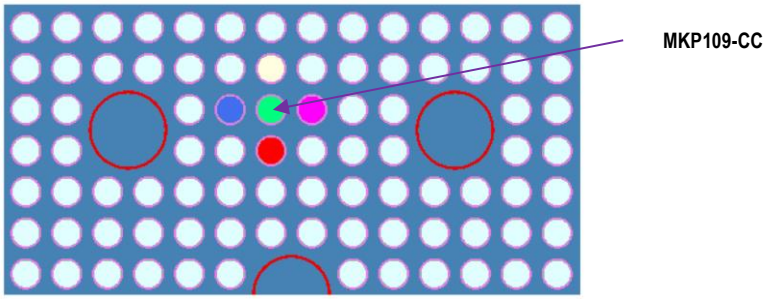

(b) ½ assembly for Calvert Cliffs MKP109-CC sample model

Figure 6. Illustrations of 2D TRITON depletion models for PWR assemblies.

3.2.3 Results

A summary of the C/E nuclide concentration ratios is presented in Table 5 for 40 of the important nuclides listed in Table 1. The mean C/E values over all measurements that are available for a specific nuclide are shown, along with the corresponding standard deviation (σ). The C/E results presented herein correspond to a sample burnup that was normalized to the reported measured ^{148}Nd for the large majority of the samples for which this burnup indicator fission product was measured. The burnup normalization approach is similar to that documented in detail in previous validation studies [8, 9].

For the major actinides ^{235}U and ^{239}Pu, experimental data are available for all 92 measured samples. However, this is not the case for fission products, especially for measurements performed under old experiments, which considered mainly actinides. Table 5 also shows C/E values previously reported for the same samples and measured nuclides that were calculated using SCALE 6.1 and the 238-group ENDF/B-VII.0 cross section library [38].

The major actinides ^{235}U and ^{239}Pu are on average well predicted, within 1.1% (σ=3.6%) and 1.9% (σ=4.1%) of the measurements. All uranium and plutonium nuclides are predicted on average within 4% compared to the experiments, except for ^{234}U. For the latter, the larger difference is mainly due to uncertainty in the initial concentration of this nuclide in the fresh fuel; the final content of this nuclide is highly dependent on the initial concentration, which is typically low (<0.05wt% ^{234}U/U) for LWR fuel and is often unreported [11]. The minor actinides are also well predicted on average, within 7% of the measurement, although in this case there is a larger variability (σ>10%) in the C/E data around the average value.

Table 5 shows generally similar results from SCALE 6.1/ENDF/B-VII.0 and SCALE 6.2.4/ENDF/B-VII.1. However, prediction is improved for a series of actinides and fission products when using SCALE 6.2.4 with ENDF/B-VII.1 cross section data. On average, the comparison between previous and current results shows no significant change for the uranium nuclides, while a significant improvement in plutonium nuclide predictions is noted, particularly in ^{239}Pu and ^{238}Pu, for which the average C/E improves by 2.2 and 7.6%, respectively. Changes in plutonium nuclides impact the calculation of nuclide contents in the higher actinides americium and curium.

A significant part of the observed differences in nuclide predictions when comparing SCALE 6.1/ENDF/B-VII.0 and SCALE 6.2.4/ENDF/B-VII.1 is likely due to differences in the evaluated nuclear data (ENDF/B-VII.1 vs. ENDF/B-VII.0), and it is less likely due to differences in the SCALE codes used, since the underlying computational methods in SCALE have not changed significantly. However, a notable change is the different energy group structure in the MG cross section library used with the NEWT neutron transport solver in SCALE 6.2.4/TRITON. This new 252-group library has refined energy binning in the plutonium resonance region compared to the 238-group library in SCALE 6.1. Improvements were also made in the cross section self-shielding methods used to generate the 252-group library for SCALE 6.2 [44]. Although it is not the purpose of this report to thoroughly investigate the sources of the differences between the two SCALE versions and the nuclear data used, it should be mentioned that the significant improvement in ^{238}Pu is attributed [45] mostly to the significant change in its (n,γ) cross section between ENDF-B/VII.0 and ENDF-B/VII.1, as illustrated in Figure 7a. On the other hand, some of the observed differences in the calculated $^{153\text{-}155}$Eu and ^{155}Gd (stable nuclide, product of ^{155}Eu β-decay) were noted to result from changes in the ^{153}Eu (n,γ) cross section (Figure 7b) [45].

Table 5. Comparison experiment–calculation (C/E) for PWR nuclide concentrations.

Nuclide	No. of samples	Application [a]	SCALE 6.2.4 ENDF/B-VII.1		SCALE 6.1 ENDF/B-VII.0		Comparison of $(C/E)_{avg}$	
			$(C/E)_{avg}$ [b]	σ [c]	$(C/E)_{avg}$	σ	mean	σ
^{234}U	55	BC, WM	1.127	0.173	1.124	0.176	0.003	0.247
^{235}U	92	BC, WM	1.013	0.036	1.012	0.035	0.001	0.050
^{236}U	77	BC, WM	0.981	0.034	0.981	0.035	0.000	0.049
^{238}U	92	BC, WM	0.999	0.004	0.999	0.004	0.000	0.006
^{238}Pu	77	BC, RS, WM	0.959	0.074	0.883	0.059	0.076	0.095
^{239}Pu	92	BC, RS, WM	1.019	0.034	1.041	0.035	-0.022	0.049
^{240}Pu	92	BC, RS, WM	1.005	0.035	1.022	0.034	-0.017	0.049
^{241}Pu	92	BC, WM	0.978	0.047	0.986	0.045	-0.008	0.065
^{242}Pu	91	BC, WM	0.959	0.064	0.941	0.061	0.018	0.088
^{237}Np	36	BC, WM	1.024	0.199	1.039	0.195	-0.015	0.279
^{241}Am	39	BC, RS, WM	1.043	0.192	1.102	0.207	-0.059	0.282
^{243}Am	38	BC, WM	0.933	0.125	1.029	0.140	-0.096	0.188
^{244}Cm	57	RS	0.987	0.113	0.956	0.111	0.031	0.158
^{245}Cm	24	BC, WM	0.987	0.150	0.985	0.156	0.002	0.216
^{246}Cm	14	RS	0.930	0.224	0.956	0.255	-0.026	0.340
^{90}Sr	15	RS, WM	0.991	0.066	0.991	0.069	0.000	0.096
^{99}Tc	20	RS, WM	1.164	0.158	1.152	0.154	0.012	0.221
^{101}Ru	7	BC	1.056	0.113	1.058	0.123	-0.002	0.167

Table 5. Comparison experiment–calculation (C/E) for PWR nuclide concentrations (continued).

Nuclide	No. of samples	Application [a]	SCALE 6.2.4 ENDF/B-VII.1		SCALE 6.1 ENDF/B-VII.0		Comparison of $(C/E)_{avg}$	
			$(C/E)_{avg}$ [b]	σ [c]	$(C/E)_{avg}$	σ	mean	σ
^{106}Ru	31	RS	1.059	0.218	1.079	0.227	-0.020	0.314
^{103}Rh	8	BC	1.115	0.106	1.091	0.109	0.024	0.152
^{109}Ag	6	BC	1.764	0.683	1.773	0.746	-0.009	1.012
^{125}Sb	18	RS	1.988	0.450	1.996	0.466	-0.008	0.648
^{133}Cs	10	BC	1.023	0.017	1.019	0.017	0.004	0.024
^{134}Cs	59	RS	0.898	0.070	0.930	0.071	-0.032	0.100
^{135}Cs	16	WM	1.021	0.036	1.027	0.037	-0.006	0.051
^{137}Cs	73	BI, RS, WM	0.989	0.032	0.993	0.031	-0.004	0.044
^{143}Nd	36	BC	1.008	0.021	1.008	0.032	0.000	0.038
^{145}Nd	36	BC	1.002	0.011	0.995	0.022	0.007	0.025
^{148}Nd	77	BI	1.000	0.003	1.006	0.014	-0.006	0.014
^{144}Ce	32	RS	0.968	0.075	0.979	0.081	-0.011	0.110
^{147}Sm	24	BC	1.009	0.032	1.016	0.034	-0.007	0.047
^{149}Sm	20	BC	1.013	0.061	1.019	0.062	-0.006	0.087
^{150}Sm	24	BC	1.009	0.028	1.008	0.032	0.001	0.042
^{151}Sm	24	BC	0.972	0.042	0.979	0.044	-0.007	0.061
^{152}Sm	24	BC	1.010	0.035	1.016	0.037	-0.006	0.051
^{151}Eu	12	BC	0.886	0.190	0.893	0.198	-0.007	0.274
^{153}Eu	19	BC	0.965	0.030	0.991	0.031	-0.026	0.043
^{154}Eu	44	RS	1.066	0.107	1.042	0.104	0.024	0.149
^{155}Eu	11	BC	0.977	0.077	0.956	0.077	0.021	0.109
^{155}Gd	19	BC	0.936	0.142	0.916	0.144	0.020	0.202

[a] BC=burnup credit, BI=burnup indicator, RS=radiation shielding, WM=waste management
[b] calculated as $(C/E)avg = [\Sigma(C/E)_i]/N$, where *i* is the measurement index, and *N* is the total number of measurements for the considered nuclide
[c] standard deviation

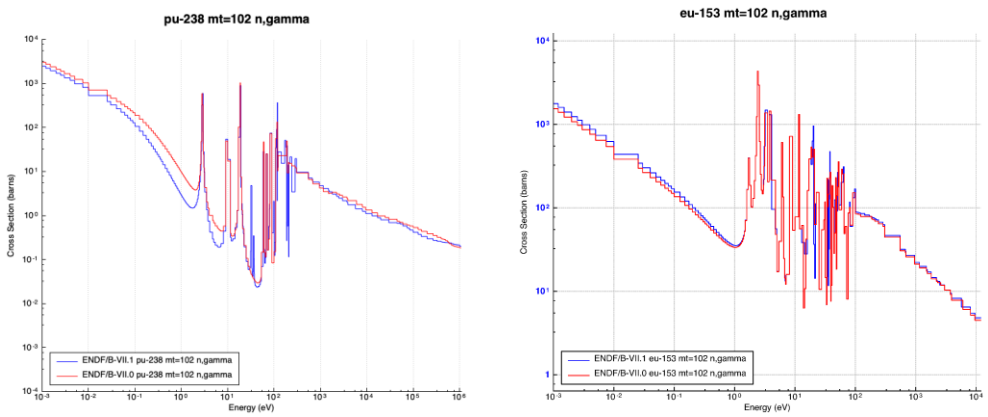

(a) change in (n, γ) cross section for ^{238}Pu **(b) change in (n, γ) cross section for ^{153}Eu**

Figure 7. Change in (n,γ) cross section between ENDF/B-VII.0 and ENDF/B-VII.1 for ^{238}Pu and ^{153}Eu.

No dependence on burnup was observed for the calculated bias in the nuclide concentrations under consideration, as exemplified in Figures 8 and 9 for ^{235}U and ^{239}Pu. These two figures show the C/E-1 value in % as function of burnup for all considered samples, with different colors being used to indicate the origin of the measured fuel by reactor name. The error bars account only for the reported measurement uncertainties; they do not include any computational uncertainty. The value and significance of the reported measurement uncertainties differ greatly among measurement programs, and in some cases, they may reflect only the mass spectrometry instrument precision or general laboratory experience in analyzing fuel samples. Recent experimental programs were specifically designed to provide high-quality RCA data for use in code validation. These programs account for the reported measurement uncertainties in all the steps of the experiment, including fuel sample dissolution, calibration, spectrometry, and others. A detailed general discussion of the impact of experimental data uncertainties on nuclide inventories calculations for PWR spent fuel can be found in work by Gauld et al. [11] . Given the inconsistent reporting of measurement uncertainties in different experimental programs, the average C/E data shown in Table 5 have not been weighted by the available measurement uncertainties. The 2σ bands shown in Figures 8 and 9 are based on the standard deviation (σ) as calculated for the individual C/E data sets for these two nuclides. As observed, the large majority of the individual C/E points are contained within the 2σ bands.

The PWR nuclide inventory validation results presented herein can serve as a technical basis for performing application-specific bias and uncertainty assessments for integral metrics of interest (e.g. decay heat, eigenvalue, dose) for which the considered nuclides are important contributors. This approach would require application-specific methods to propagate the available nuclide bias and uncertainties using either bounding or best-estimate methods. As an example, this approach was applied in burnup credit for criticality analysis [13, 14].

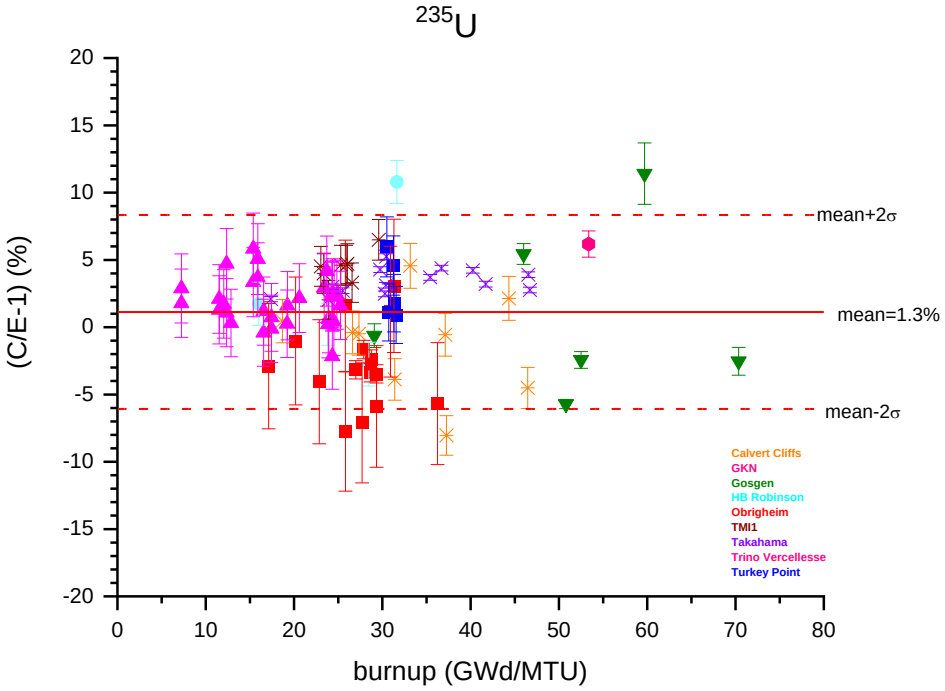

Figure 8. Comparison calculation-experiment vs. burnup for ^{235}U in PWR spent fuel.

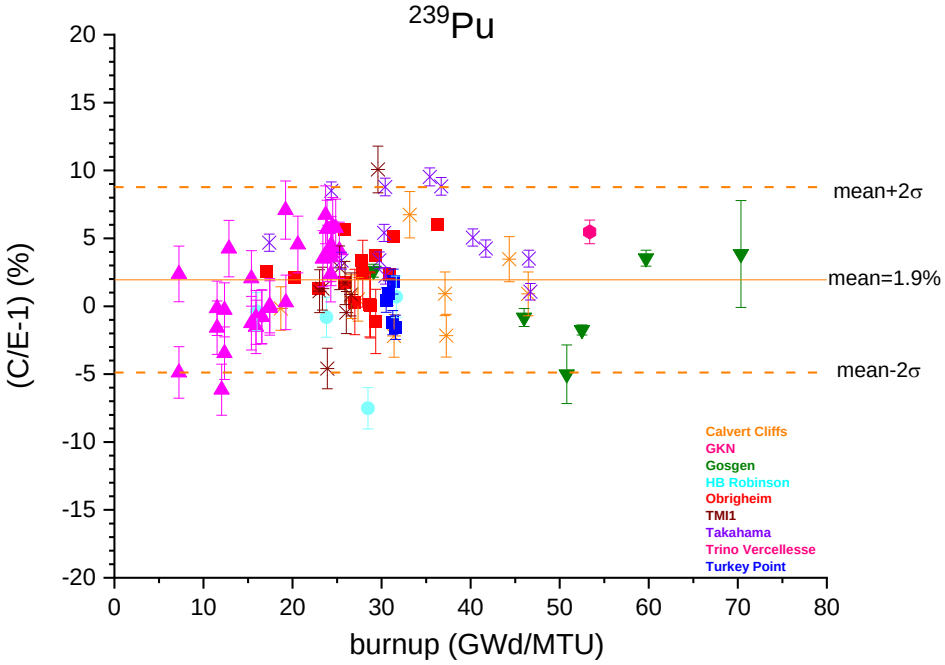

Figure 9. Comparison calculation-experiment vs. burnup for ^{239}Pu in PWR spent fuel.

3.3 BWR

3.3.1 Experimental Data

The summary of the BWR RCA data considered in this validation report is presented in Table 6. The same data set has been used for validation studies with SCALE 6.2.2 and ENDF/B-VII.1 nuclear data [22]. This RCA set includes data for 77 samples selected from 23 fuel rods that were irradiated in six BWRs operated in five countries: Belgium, Japan, Sweden, Switzerland, and United States. The fuel rods were selected from assemblies with different lattices (6×6, 8×8, 9×9, 10×10) and assembly designs (SVEA-64, SVEA-96, GE-11, and GE-14). Of these 77 samples, 26 were selected from UO_2-Gd_2O_3 fuel rods with 3.0 to 5.0% Gd_2O_3 loading. The considered samples include enrichments ranging from 2.1 to 4.94% ^{235}U, except for three of the samples that were selected from the natural uranium blanket regions of fuel rods. The total number of samples discussed herein is 76, since one of the samples with natural uranium enrichment was excluded because the available modeling data were deemed insufficient for a reliable 2D simulation. The burnups in the 76 samples range from 4.2 to 68.4 GWd/MTU, and the average void fraction during irradiation at the sample location is in the 0–74% range.

3.3.1.1 Fuel samples characteristics

The distribution of burnup as function of enrichment for these BWR samples is illustrated in Figure 10; the colors indicate fuel's origin by reactor name. The histogram of the enrichments and the histogram of the burnups for the considered samples are provided in Figure 11. Almost 80% of the samples have assembly-average enrichments between 3.0 and 4.0% ^{235}U; 11 samples have enrichments between 4.0 and 5.0% ^{235}U. Approximately half of the samples have burnups lower than 40 GWd/MTU, and the other half covers higher burnups ranging between 40 and 68 GWd/MTU. Also, almost half of the samples have average void fractions greater than 50% (see Figure 12).

Table 7 summarizes the number of BWR measurements available for nuclides important for burnup credit, decay heat, and shielding applications, as applicable to the 76 samples considered in this validation study. Uranium and plutonium nuclide measurements are available for all BWR samples under consideration.

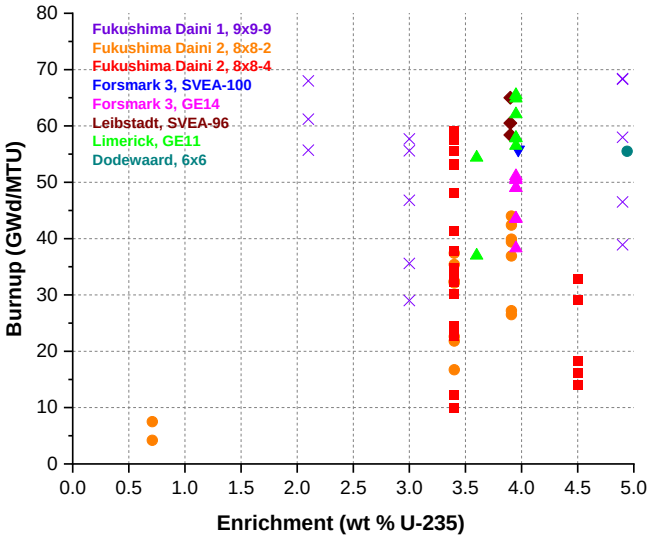

Figure 10. Burnup distribution vs. enrichment for the measured BWR spent fuel.

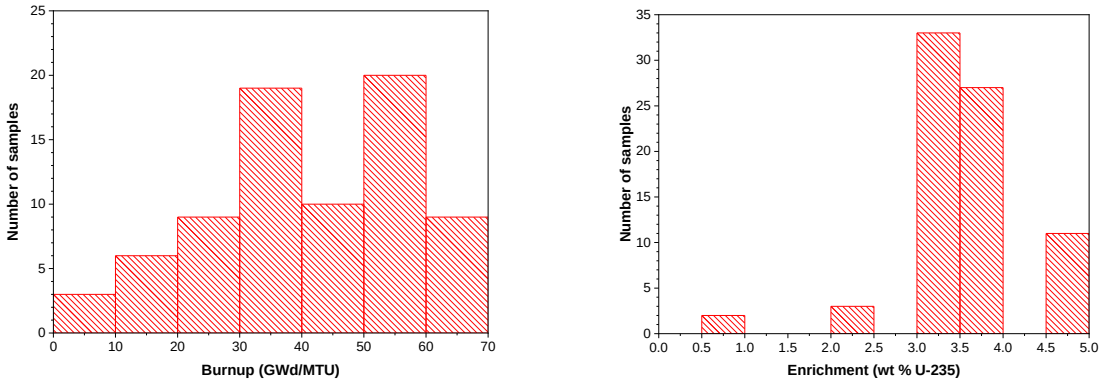

Figure 11. Enrichment and burnup distribution histograms for the measured BWR spent fuel.

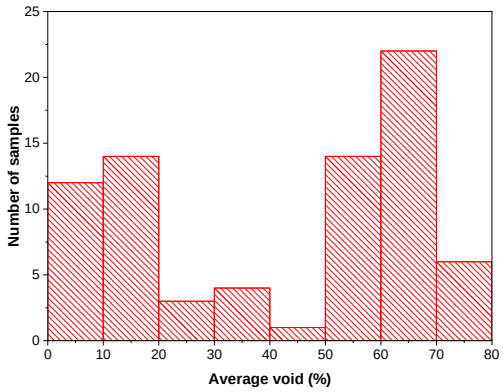

Figure 12. Average void fraction distribution histogram for the measured BWR spent fuel.

Table 6. Summary of BWR RCA data used for validation.

Reactor	Country	Measurement laboratory [a]	Experimental Program [b]	Assembly lattice	Enrichment [c] (% ^{235}U)	No. of samples / fuel rods	Burnup (GWd/MTU)
Dodewaard	Belgium	SCK·CEN, PSI	ARIANE	6 × 6	4.941	1/1	55.5
Forsmark 3	Sweden	Studsvik	Studsvik CSN	10 × 10 (SVEA-96) 10 × 10 (GE-14)	3.97 3.95	1/1 8/1	55.8 38.3–51.1
Fukushima Daini 1	Japan	JNES	JNES	9 × 9-9	2.1, 4.9, 3.0 (Gd)	13/5	35.6–68.4
Fukushima Daini 2	Japan	JAERI	JAERI	8 × 8-4 8 × 8-2	3.4, 4.5, 3.4 (Gd) 0.71,3.9, 3.4 (Gd)	25/8 18/2	9.4–59.1 4.2–44.0
Leibstadt	Switzerland	Studsvik	MALIBU [g]	10 × 10 (SVEA-96)	3.9	3/1	58.4–65.0
Limerick	US	GE-VNC	DOE YMP	9 × 9 (GE-11)	3.95, 3.6 (Gd)	8/3	37.0–65.5

[a] GE-VNC = General Electric Vallecitos Nuclear Center; JAERI = Japan Atomic Energy Research Institute (now Japan Atomic Energy Agency); JNES = Japan Nuclear Energy Safety (now Japan Regulation Authority)

[b] ARIANE and MALIBU were international experimental programs coordinated initially by Belgonucleaire, Belgium, and later managed by SCK-CEN; CSN=Consego de Securidad Nuclear (Spanish Nuclear Safety Council); DOE YMP = US Department of Energy Yucca Mountain Project

[c] Enrichments for UO_2-$Gd2O_3$ fuel rods are identified by *(Gd)* following the enrichment value.

Table 7. Number of BWR measurements per nuclide.

Nuclide	No. of samples	Application[a]
^{234}U	76	BC, WM
^{235}U	76	BC, WM
^{236}U	76	BC, WM
^{238}U	76	BC, WM
^{238}Pu	76	BC, RS, WM
^{239}Pu	76	BC, RS, WM
^{240}Pu	76	BC, RS, WM
^{241}Pu	76	BC, WM
^{242}Pu	76	BC, WM
^{237}Np	29	BC, WM
^{241}Am	62	BC, RS, WM
^{243}Am	62	BC, WM
^{242}Cm	48	RS
^{243}Cm	48	BC, WM
^{244}Cm	51	RS
^{95}Mo	23	RS, WM
^{99}Tc	16	RS, WM
^{101}Ru	14	BC
^{103}Rh	15	BC
^{109}Ag	15	BC
^{133}Cs	16	BC
^{137}Cs	42	BI, RS, WM
^{143}Nd	50	BC
^{145}Nd	50	BC
^{146}Nd	50	BC
^{148}Nd	75	BI
^{147}Sm	35	BC
^{149}Sm	32	BC
^{150}Sm	34	BC
^{151}Sm	35	BC
^{152}Sm	35	BC
^{151}Eu	15	BC
^{153}Eu	25	BC
^{155}Eu	25	BC
^{155}Gd	25	BC

[a] as listed in Table 1; BC=burnup credit, BI=burnup indicator, RS=radiation shielding, WM=waste management

3.3.2 Models

The 2D depletion models used for simulating the BWR sample irradiation histories are similar to those applied in previous validation studies [22, 23]. These models were developed with the Polaris LWR

lattice physics code in SCALE [26]. Polaris employs the method of characteristics (MOC) for solving the neutron transport equation, and provides an input format that allows users to set up LWR lattice models with a minimal amount of input compared to TRITON [42], which was designed to enable lattice physics for general geometry configurations. Within Polaris, the ORIGEN depletion and decay code [43] is coupled with the MOC neutron transport solver to simulate the time-dependent fuel irradiation history.

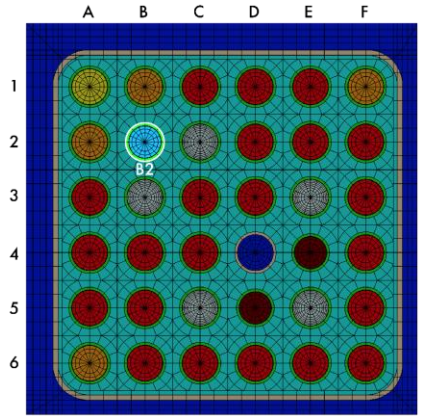

(a) Dodewaard 6 × 6 assembly

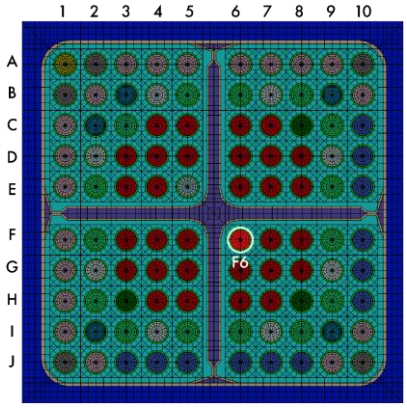

(b) Forsmark Unit 3 SVEA-100 assembly

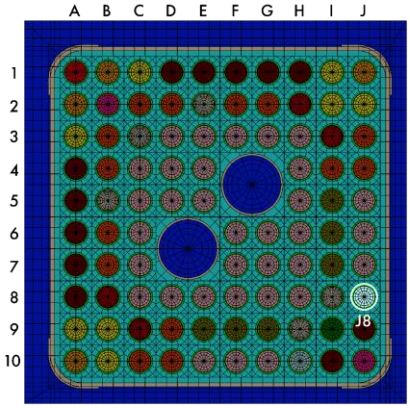

(c) Forsmark Unit 3 GE-14 assembly

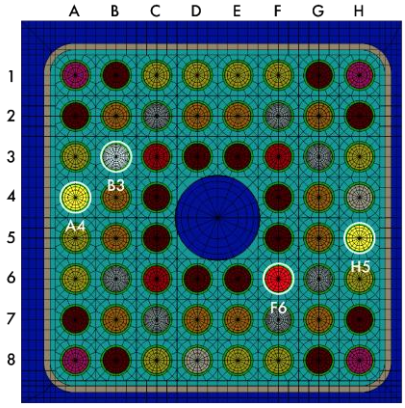

(d) Fukushima Daini-2 8 × 8-4 assembly

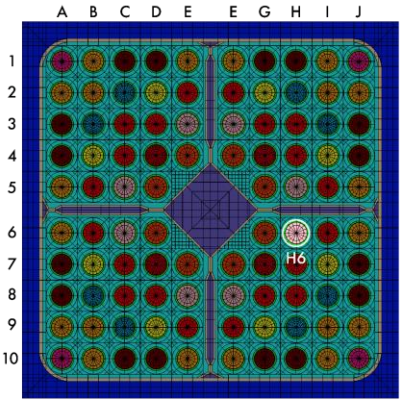

(e) Leibstadt SVEA-96 assembly

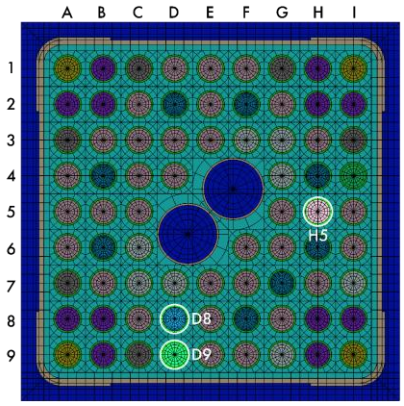

(f) Limerick GE-11 assembly

Figure 13. Illustrations of 2D Polaris depletion models for BWR assemblies.

All BWR depletion simulations in this study were performed with Polaris in SCALE version 6.2.4 using the 56-group ENDF/B-VII.1 cross section library. Selected 2D models are illustrated in Figure 13 for six

of the seven assemblies; depleted mixtures and other materials are mapped by unique colors in these illustrations, and the measured fuel rods are highlighted.

3.3.3 Results

A summary of the C/E nuclide concentration ratios is presented in Table 8 for 35 of the important nuclides listed in Table 1. The mean C/E values over all measurements available for a specific nuclide are shown, along with the corresponding standard deviation. The C/E results presented herein correspond to calculations that used the reported sample burnup.

The major actinides ^{235}U and ^{239}Pu are on average well predicted, within 3% of the measurement; however, there is a large spread of the two individual C/E values around the mean as indicated by the σ values of 11.1 and 8.6%, respectively. All uranium and plutonium nuclides are predicted on average within 7% compared to the experiment. The minor actinides, except for ^{243}Cm, are predicted within 10% of the measurement.

Of the 17 fission products considered, 15 that are important for burnup credit are on average well predicted, within 7% of the experiment. The exceptions are ^{151}Eu, which is predicted within 12% (σ=20%) and ^{109}Ag, which is overpredicted by 34% (σ=39%). The latter is a metallic fission product that is generally very difficult to measure and for which the measurement uncertainties are likely underreported [11].

Table 8. Comparison experiment–calculation for BWR nuclide concentrations.

Nuclide	No. of samples	Application [a]	SCALE 6.2.4 ENDF/B-VII.1	
			$(C/E)_{avg}$ [b]	σ [c]
^{234}U	76	BC, WM	1.039	0.128
^{235}U	76	BC, WM	1.027	0.111
^{236}U	76	BC, WM	1.017	0.047
^{238}U	76	BC, WM	0.999	0.003
^{238}Pu	76	BC, RS, WM	1.063	0.206
^{239}Pu	76	BC, RS, WM	0.974	0.085
^{240}Pu	76	BC, RS, WM	0.999	0.088
^{241}Pu	76	BC, WM	0.941	0.114
^{242}Pu	76	BC, WM	0.985	0.168
^{237}Np	29	BC, WM	0.986	0.120
^{241}Am	62	BC, RS, WM	0.991	0.167
^{243}Am	62	BC, WM	1.053	0.344
^{242}Cm	48	RS	0.906	0.679
^{243}Cm	48	BC, WM	0.632	0.526
^{244}Cm	51	RS	0.983	0.456
^{95}Mo	23	RS, WM	1.020	0.077
^{99}Tc	16	RS, WM	1.262	0.156
^{101}Ru	14	BC	1.058	0.134
^{103}Rh	15	BC	1.066	0.090
^{109}Ag	15	BC	1.336	0.386
^{133}Cs	16	BC	0.970	0.072
^{137}Cs	42	BI, RS, WM	0.968	0.061
^{143}Nd	50	BC	1.039	0.038
^{145}Nd	50	BC	1.022	0.030
^{146}Nd	50	BC	1.001	0.025
^{148}Nd	75	BI	1.005	0.027
^{147}Sm	35	BC	0.991	0.079
^{149}Sm	32	BC	0.921	0.120
^{150}Sm	34	BC	1.033	0.067
^{151}Sm	35	BC	0.974	0.116
^{152}Sm	35	BC	1.055	0.065
^{151}Eu	15	BC	0.880	0.208
^{153}Eu	25	BC	1.037	0.034
^{155}Eu	25	BC	1.009	0.161
^{155}Gd	25	BC	1.055	0.110

[a] BC=burnup credit, BI=burnup indicator, RS=radiation shielding, WM=waste management
[b] calculated as $(C/E)avg = [\Sigma(C/E)_i]/N$, where *i* is the measurement index, and *N* is the total number of measurements for the considered nuclide
[c] standard deviation

3.4 DISCUSSION

Validation of the depletion capabilities and associated ENDF/B-VII.1 nuclear data in SCALE 6.2.4 to predict nuclide inventories in PWR and BWR spent nuclear fuel was demonstrated based on RCA data for up to 40 nuclides per sample, for 92 PWR and 76 BWR fuel sample measurements. These measurements cover initial enrichments up to 5% ^{235}U and burnups as high as 70 GWd/MTU, although most of the considered BWR samples and the majority of the PWR samples have less than 40 GWd/MTU burnup. The comparison calculation-experiment shows on average a good agreement for many of the nuclides important to burnup credit, decay heat, and radiation shielding applications, considering the uncertainties associated with the experimental data. The histograms of the C/E data for the two major actinides ^{235}U and ^{239}Pu are presented in Figure 14 for PWR samples and in Figure 15 for BWR samples. The mean C/E value for ^{235}U is 1.013 (σ=0.036) for PWR samples and 1.027 (σ=0.111) for BWR samples, whereas for ^{239}Pu, the average C/E is 1.019 (σ=0.034) for PWR samples and 0.974 (σ=0.085) for BWR samples. A greater variability around the mean C/E is noticed for the BWR results. Though this is partially due to experimental uncertainties, as in the PWR case, significant variability may result from insufficient or missing modeling data required to adequately represent the neutronic environment, such as void fraction at the sample level or assembly exposure to control blades during irradiation. Compared to prediction of integral quantities such as eigenvalue or assembly decay heat, for which the intra-assembly flux spectrum and neutron moderation as function of radial and axial location may not play a primary role, for analysis of RCA data that is obtained on fuel samples at pellet size level, the local neutronic environment is very important.

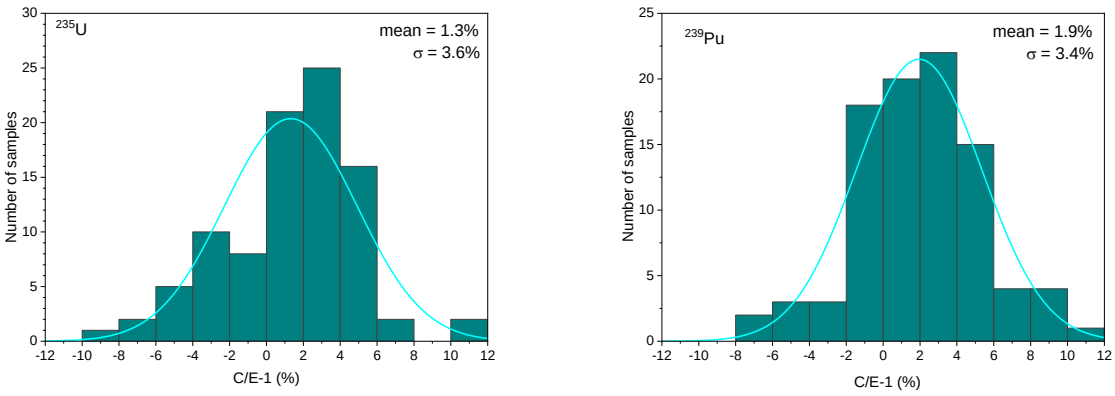

Figure 14. Comparison calculation-experiment vs. burnup for ^{235}U and ^{239}Pu in PWR samples.

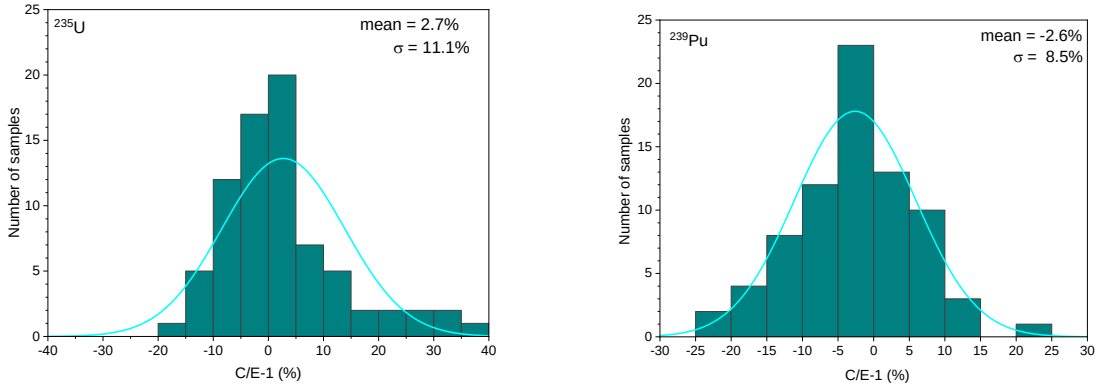

Figure 15. Histogram plots for ^{235}U and ^{239}Pu calculation-experiment comparisons for BWR samples.

Comparison of C/E results obtained with SCALE 6.2.4/ENDF/B-VII.1 and those obtained with SCALE 6.1/ENDF/B-VII.0 for PWR samples when using a consistent validation basis (see Table 5) shows average C/E differences of less than 2% for most actinides and fission products, with practically no differences for uranium nuclides and most of the measured fission products. Notably, differences greater than 2% that are also associated with prediction improvement (C/E closer to 1) are seen for actinides ^{238}Pu, ^{239}Pu, ^{241}Am, and ^{243}Am. As previously mentioned, a large source of the difference in these actinides predictions was identified as the change in ^{238}Pu capture cross section between ENDF/B-VII.0 and ENDF/B-VII.1. A complete assessment of the sources in the computational bias or the uncertainties in calculated nuclide content that are due to uncertainties in either measurement or calculation is beyond the informative goal of the present report. Related detailed discussions are available in other publications [11, 18, 23, 45].

4. DECAY HEAT

4.1 FUEL ASSEMBLY MEASUREMENTS

Decay heat generated in spent nuclear fuel, also known as *residual decay heat*, is the recoverable energy released from the decay of radionuclides present in fuel upon its discharge from the reactor. Driven by the nuclide composition in fuel at the end of irradiation, decay heat for a spent fuel assembly depends primarily on burnup, cooling time (from assembly discharge to a time point of interest), enrichment, fuel design, reactor type, and operating history of the assembly. Decay heat is a critical parameter for the design, safety, and licensing analyses of used nuclear fuel storage, transportation, and repository systems.

The validation of SCALE 6.2.4 with ENDF/B-VII.1 data for decay heat analysis of LWR spent fuel presented in this report is based on a set of full-assembly decay heat experimental data that have been used in previous validation studies [28–31, 46] and documented in detail in previous publications. For completeness, a summary of the experimental data is presented herein. More details can be found in the indicated references.

4.1.1 Experimental Data

The full-assembly decay heat experimental data considered in this report are summarized in Table 9. These data come from experiments performed in the 1980s by General Electric at the GE-Morris facility in the United States, and from experiments prior to the 2010s as conducted by SKB at the Clab interim storage facility in Sweden. The assemblies measured at GE-Morris were irradiated in reactors operated in the United States, and those measured at Clab came from Swedish reactors. The PWR data include 91 measurements performed on 42 assemblies (multiple measurements were performed on the same assembly at different cooling times) covering a burnup range of 18–51 GWd/MTU, cooling times between 4.5 and 27.7 years, and initial fuel enrichments from 2.1 to 4.0% ^{235}U. The BWR data include 145 measurements performed on 83 assemblies, covering a burnup range of 5–45 GWd/MTU, cooling times between 2.3 and 26.7 years, and initial assembly-average fuel enrichments between 1.1 and 2.9% ^{235}U.

The coverage of the considered measurements over the burnup and cooling time space is illustrated in Figure 16; the colors indicate the fuel's origin by reactor name. The histograms of the burnups and cooling times for the considered measurements are provided in Figures 17 and 18, respectively. Approximately 20% of the PWR measurements are available for cooling times of less than 10 years, and all were performed at GE-Morris on assemblies with older 14×14 and 15×15 designs. The number of BWR measurements at cooling times of less than 10 years is greater than the number of measurements for PWRs; however, the large majority of them were made on assemblies from the same reactor—Cooper—and for an old 7×7 assembly design.

Table 9. Summary of full-assembly decay heat experimental data used for validation.

Reactor type	Reactor name	Assembly lattice	Burnup (GWd/MTU)	Cooling time (years)	Enrichment (% ^{235}U)	Measurement laboratory	No. of measured assemblies	No. of measurements	Exp. relative uncertainty [a] (%)
PWR	Point Beach 2	14×14	31.9–39.4	4.5	3.4	GE-Morris	6	6	4.7
	San Onofre 1	15×15	26.5–32.4	3.0–8.2	3.9 – 4.0	GE-Morris	8	8	4.7
	Turkey Point 3	14×14	18.4–28.4	2.4–5.7	2.6	GE-Morris	4	6	5.0 – 10.0
	Ringhals 2	15×15	34.0–51.0	15.9–26.7	3.1 – 3.3	Clab	18	33	2.3 – 3.0
	Ringhals 3	17×17	19.7–47.3	12.9–25.9	2.1 – 3.4	Clab	16	38	2.2 – 4.1
BWR	Cooper	7×7	11.7–28.0	2.3–7.2	1.1 – 2.5	GE-Morris	54	81	4.7
	Dresden 2	7×7	5.3	8.1	2.1	GE-Morris	1	1	4.7
	Monticello	7×7	9.2–21.0	9.7–11.2	2.3	GE-Morris	6	13	4.7
	Oskarshamn 2	8×8	14.5–24.5	20.3–26.7	2.2	Clab	5	5	4.2 – 7.5
	Ringhals 1	8×8	21.3–44.7	12.6–23.6	2.3 – 2.9	Clab	17	45	2.5 – 5.1

[a] reported measurement uncertainty at 95% confidence level, as provided for GE-Morris experiments and for Clab experiments in [28].

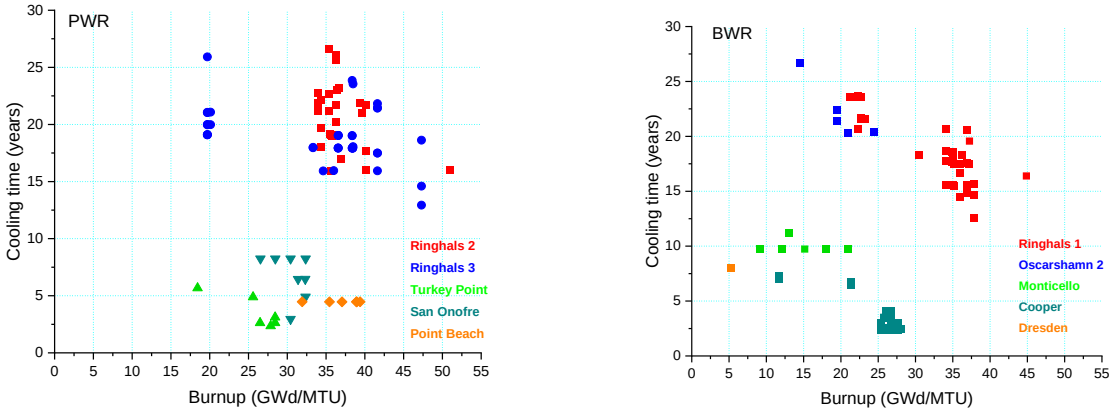

Figure 16. Burnup and cooling time distribution for the PWR and BWR assembly decay heat measurements.

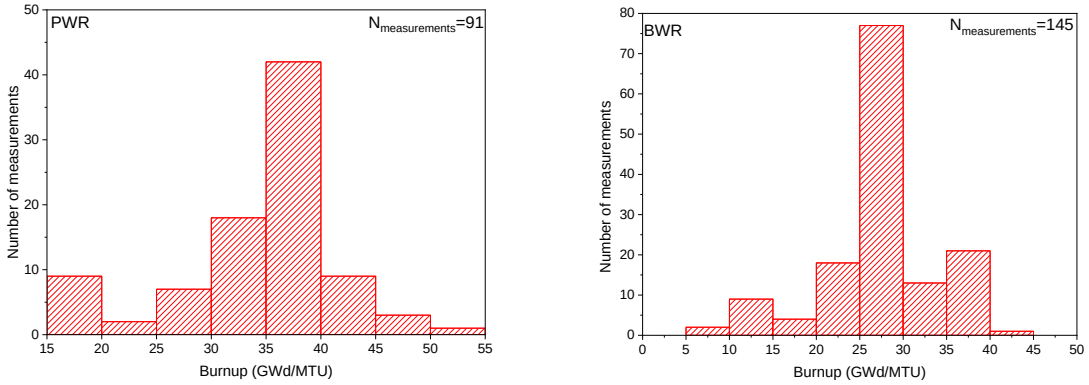

Figure 17. Burnup distribution histogram for the PWR and BWR assembly decay heat measurements.

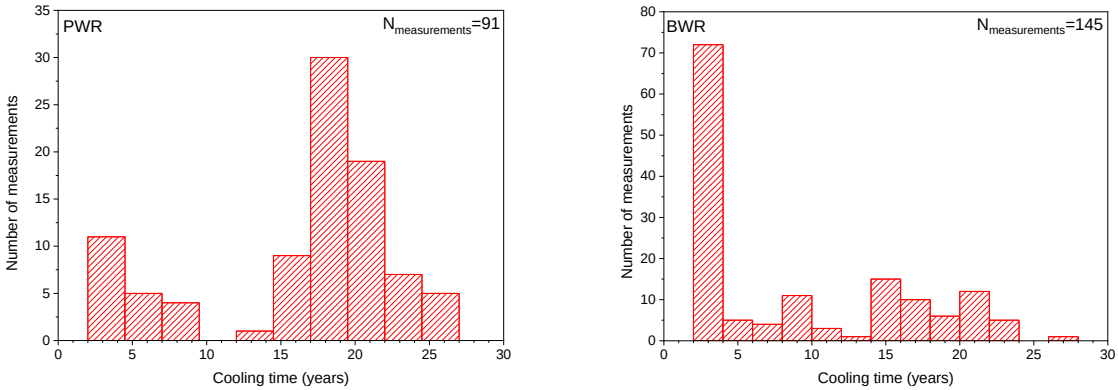

Figure 18. Cooling time distribution histogram for the PWR and BWR assembly decay heat measurements.

4.1.2 Models

The simulation methodology for determining the assembly decay heat in this study is similar to that previously used [47] and is illustrated in Figure 19. The methodology consists of two main computational steps. The first step is the generation of ORIGEN reactor libraries for the assemblies of interest. In SCALE 6.2.4, these libraries can be generated by performing 2D TRITON depletion simulations for the assembly configuration and operation history of interest; the ORIGEN reactor library is a by-product of the TRITON simulation and includes the nuclear data (cross sections as function of burnup, fission yields, and decay data) that enables burnup-dependent ORIGEN standalone simulations. Pre-generated ORIGEN reactor libraries are available in the SCALE 6.2.4 release for a variety of reactor types and assembly designs. The second step consists of ORIGEN standalone depletion and simulations, which are easily performed for LWR assemblies by using the ORIGAMI graphical user interface in SCALE 6.2.4.

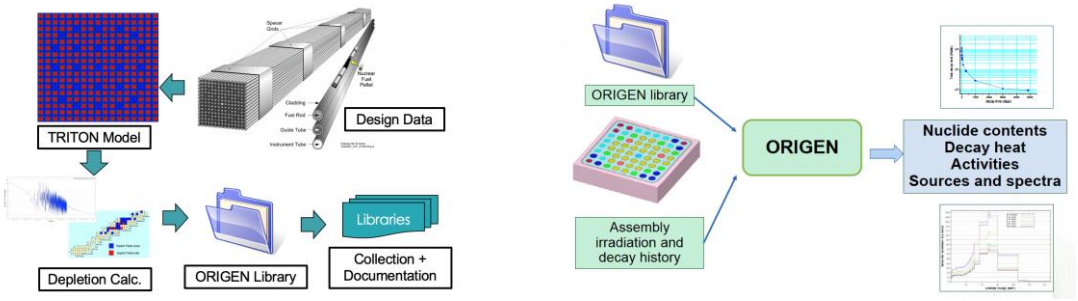

(a) generation of ORIGEN reactor library **(b) ORIGEN depletion and decay simulation**

Figure 19. Decay heat simulation methodology [47].

The modeling data used in this study were obtained from two previous publications: Gauld et al. [28] for the fuel assemblies of US origin that were measured at GE-Morris, and Ilas et al. [30] for the assemblies measured at Clab. These modeling data served to develop 2D TRITON models to generate assembly-specific ORIGEN reactor libraries for each group of the assemblies with similar characteristics listed in Table 9. The assembly-representative ORIGEN reactor libraries distributed with SCALE could have been used to provide a reliable estimate of an integral metric such as the decay heat. However, as the goal of the study was to determine best-estimate results, custom libraries were generated.

The ORIGEN libraries for the PWR assemblies were generated as a function of burnup and enrichment, whereas those for BWR assemblies were created as a function of burnup, enrichment, and coolant density. The decay heat simulations were performed with ORIGAMI using the generated ORIGEN reactor libraries and the assembly-specific data (irradiation and decay history, fuel composition and mass, cladding and spacers composition and mass) as available for each of the considered measured assemblies and each measurement. For the BWR assemblies, an assembly-average burnup and coolant density were used with the ORIGAMI simulations.

4.1.3 Results

The results are illustrated separately for PWR and BWR assemblies, given the significant differences in assembly decay heat (different assembly fuel and structure material mass) and the assembly configuration and operation (different enrichments, burnable absorbers, etc.) for the BWR assemblies, which are more heterogeneous compared to the PWR assemblies. Comparison of the calculated and measured assembly decay heat data is illustrated in Figure 20, showing a quasi-linear behavior for both reactor types. The range of the measured decay heat values is ~200–950 W for PWR assemblies and ~50–400 W for BWR assemblies.

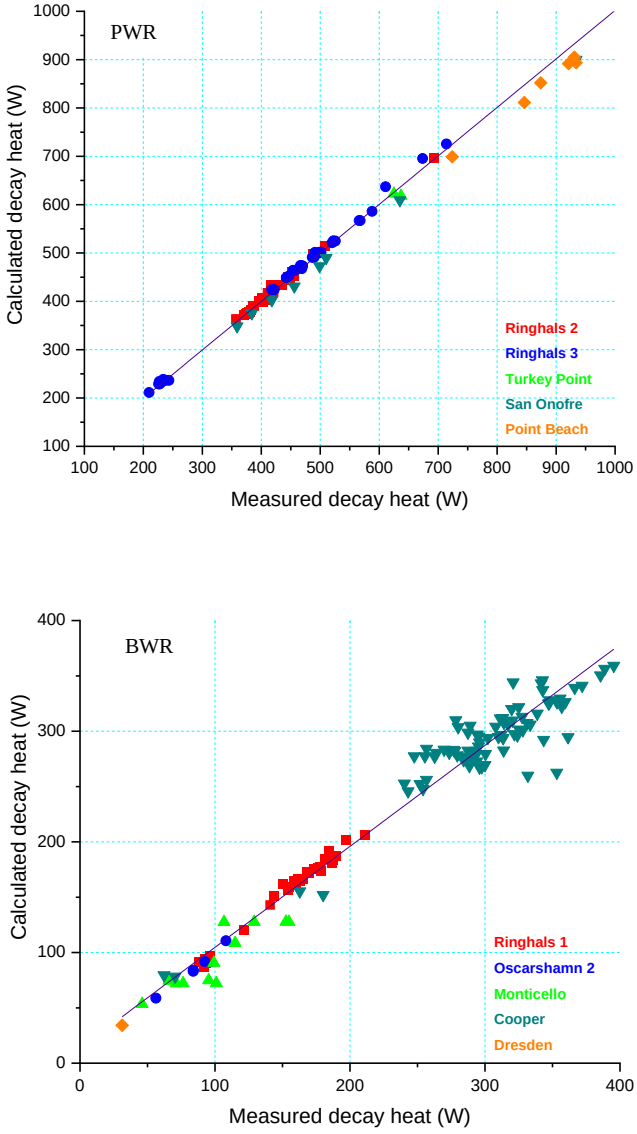

Figure 20. Comparison of calculated vs. measured assembly decay heat.

The comparison of calculated and experimental decay heat is summarized in Table 10 by reactor name and reactor type (PWR and BWR). This table shows the average and corresponding standard deviation for the C/E decay heat ratio, as well as for the difference between calculated and experimental decay heat (C-E). The number of measurements and the reported experimental uncertainty ranges are also included to illustrate the relevance of the presented results, along with the cooling time range. A good agreement is observed between calculation and experiment results for each reactor type. The predicted decay heat is on average within 1% of the experiment results (σ=1.6%) for PWRs, and it is within 2% of the experiment results (σ=7.7%) for BWRs. The same level of good agreement is also shown in the C-E difference.

Table 10. Summary of full-assembly decay heat results.

Reactor name	Reactor type	No. of measurements	% relative exp. uncert.	Cooling time (years)	C/E		C-E (W)	
					mean	σ	mean	σ
Point Beach 2	PWR	6	4.7	4.5	0.966	0.007	–29.5	6.8
Ringhals 2	PWR	33	2.3 – 3.0	15.9–26.7	1.006	0.013	2.7	5.4
Ringhals 3	PWR	38	2.2 – 4.1	12.9–25.9	1.009	0.012	4.3	6.1
San Onofre 1	PWR	8	4.7	3.0–8.2	0.961	0.011	–20.8	8.7
Turkey Point 3	PWR	6	5.0 – 10.0	2.4–5.7	1.010	0.027	17.4	28.8
Cooper	BWR	81	4.7	2.3–7.2	0.970	0.078	–11.6	22.0
Dresden 2	BWR	1	4.7	8.1	1.095	na	3.0	na
Monticello	BWR	13	4.7	9.7–11.2	0.967	0.153	–5.8	15.6
Oskarshamn 2	BWR	5	4.2 – 7.5	20.3–26.7	1.010	0.024	0.7	1.7
Ringhals 1	BWR	45	2.5 – 5.1	12.6–23.6	1.009	0.025	1.5	3.6
PWR		91		2.4–26.7	1.006	0.016	2.8	5.5
BWR		145		2.3–26.7	0.984	0.077	–6.5	18.2
PWR+BWR		236		2.3–26.7	0.993	0.062	–2.9	15.3

The assembly decay heat value is primarily driven by burnup and cooling time. No trending was identified [46] in the C/E results with either of these two parameters. The variation of the C/E values is presented in Figure 21 as function of burnup and in Figure 21 as function of cooling time.

The decay heat results obtained with SCALE 6.2.4/ENDF/B-VII.1 are expected to be generally consistent with those obtained with SCALE 6.1/ENDF/B-VII.0, except for potential impacts of changes in the evaluated data between the two ENDF/B releases. Generally, changes between SCALE 6.2.4 and SCALE 6.1 for the codes used in this analysis do not involve significant updates in the underlying methods that would be of significant consequence for decay heat estimation. A comparison of SCALE 6.2.4/ENDF/B-VII.1 decay heat results and corresponding SCALE 6.1/ENDF/B-VII.0 results is presented in Table 11 for 71 PWR cases and 50 BWR cases for which SCALE 6.1 results are available. Further results are also presented in Ilas et al. 2008 [30]. This comparison shows that, on average, the results differ by 0.6% (σ=0.5%) for PWRs and by 1.2% (σ=0.8%) for BWRs. Preliminary assessment to identify the cause of the difference indicated [46] that the change in the capture cross section of ^{238}Pu between ENDF/B-VII.0 and ENDF/B-VII.1 (see Figure 7) is the major source of the discrepancy. As noted in Section 3.2.3 (see Table 5), the prediction of ^{238}Pu in PWR spent fuel is significantly improved with SCALE 6.2.4/ENDF/B-VII.1, and it differs on average by 8% from that calculated with SCALE 6.1/ENDF/B-VII.0.

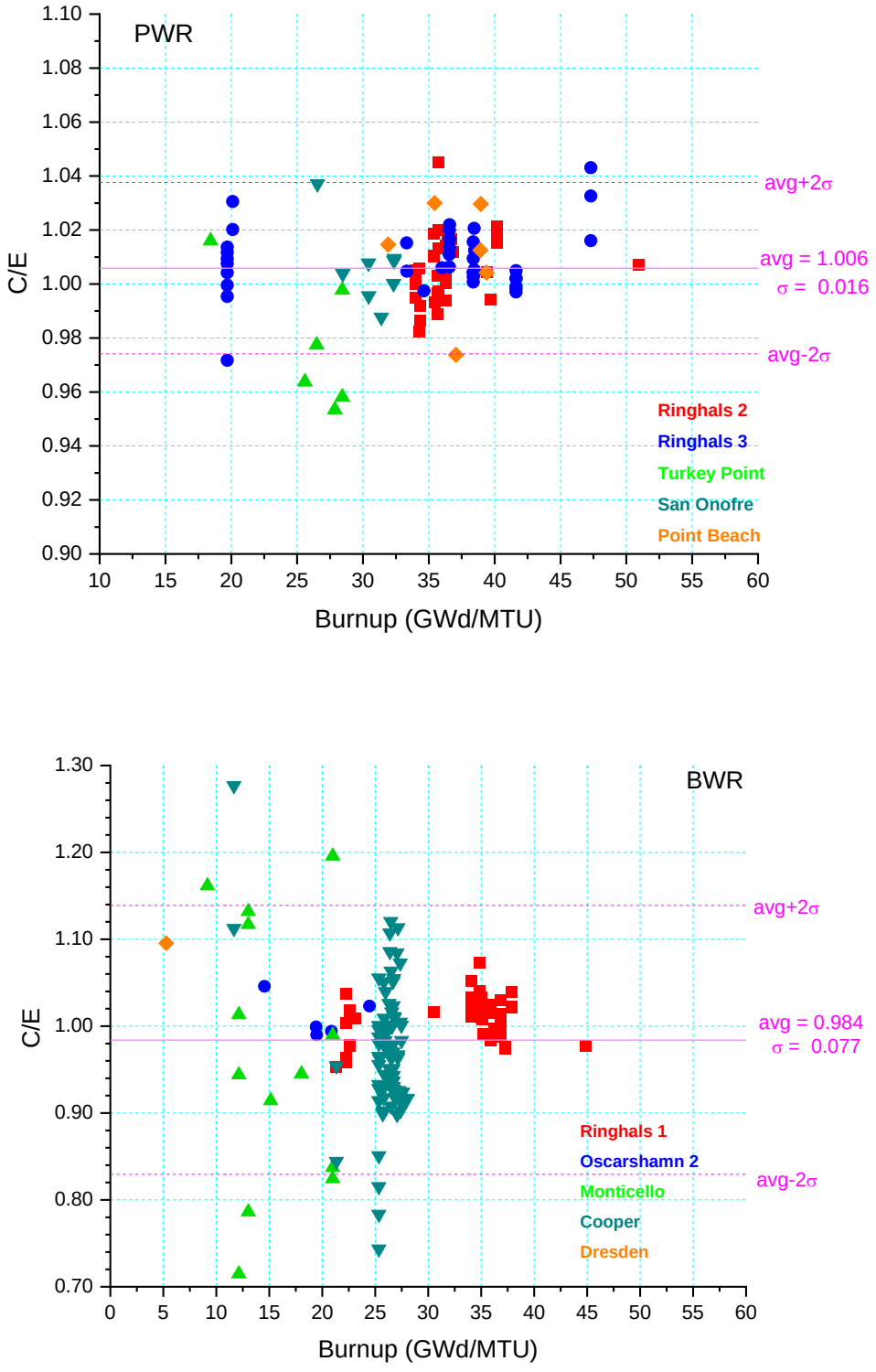

Figure 21. Decay heat calculation-experiment comparison as a function of burnup.

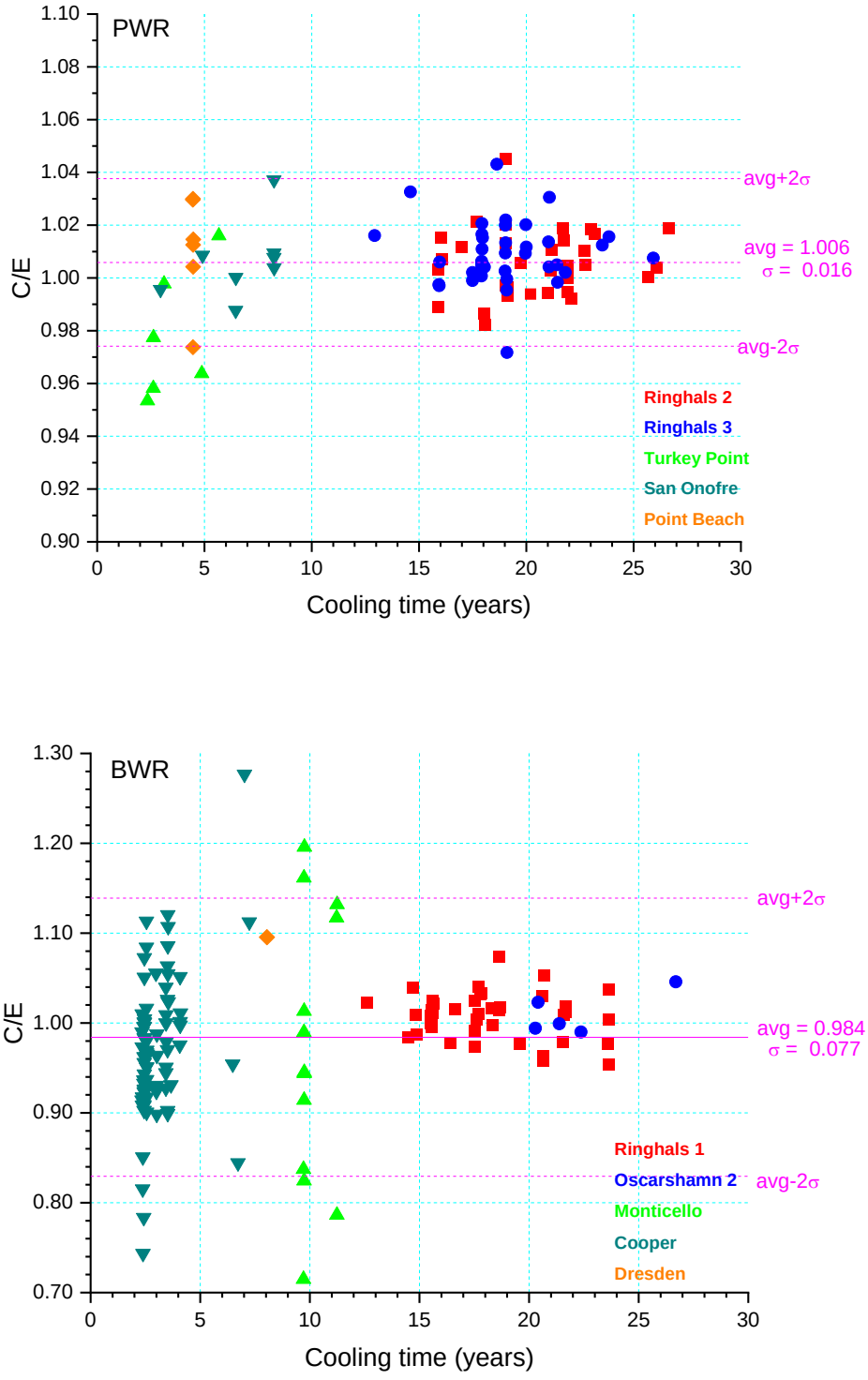

Figure 22. Decay heat calculation-experiment comparison as a function of cooling time.

Table 11. Comparison of decay heat results between SCALE 6.2.4/ENDF/B-VII.1 and SCALE 6.1/ENDF/B-VII.0 [30] [46].

Reactor name	Reactor type	No. of meas.	Cooling time (year)	C/E SCALE 6.2.4 ENDF/B-VII.1		C/E SCALE 6.1 ENDF/B-VII.0		C/E difference (SCALE6.2.4/VII.1) – (SCALE6.1/VII.0)	
				mean	σ	mean	σ	mean	σ
Ringhals 2	PWR	33	15.9 – 26.7	1.006	0.013	0.998	0.012	0.008	0.003
Ringhals 3	PWR	38	12.9 – 25.9	1.009	0.012	1.005	0.011	0.004	0.006
Ringhals 1	BWR	45	12.6 – 23.6	1.009	0.025	0.999	0.024	0.010	0.002
Oskarshamn 2	BWR	5	20.3 – 26.7	1.010	0.024	0.975	0.020	0.036	0.007
PWR		71	15.9 – 25.9	1.008	0.012	1.013	0.013	0.006	0.005
BWR		50	12.6 – 26.7	1.009	0.024	1.002	0.012	0.012	0.008
PWR+BWR		121	12.6 – 26.7	1.008	0.018	1.000	0.017	0.009	0.007

4.2 FISSILE MATERIALS IRRADIATIONS

4.2.1 Experimental Data

Full-assembly decay heat experiments are not feasible for very short cooling times up to ~10^5 s that are of interest for evaluation of postulated loss-of-coolant accident scenarios. Experiments for determining the energy release for very short cooling times following reactor shutdown generally involve a very short time (seconds) of irradiation in a neutron flux of a small amount of a fissile material (foil), followed by measurements to determine the energy dissipated after fission. These types of experiments are also known as *pulse* fission experiments and are generally based on two type of measurement methods:
(a) calorimeter measurements to directly determine decay heat, and (b) spectroscopy measurements to determine gamma and beta spectra that are further used to derive the associated decay heat from the individual gamma and beta energy components.

The experimental data used for validation herein were obtained from experiments designed to determine the energy release from fission of ^{233}U, ^{235}U, ^{238}U, ^{239}Pu, ^{241}Pu, and ^{232}Th, as presented in detail in by Gauld et al. [28] and summarized in Table 12. For each of the considered nuclides, the table specifies the measurement laboratory, the year the experiment was performed, the type of measurement (spectrometry, calorimetry), and the range of cooling time. These measurement results are typically reported as (MeV/fission), and the irradiation times of the small fissile material samples are usually much smaller (order of seconds) than the cooling times at which the measured decay heat is reported. Notably, the Lowell measurements cover lower cooling time values than the other considered experiments, going down to less than 1s following fission. Overall, these experiments cover cooling times from 0.2 s to 11 h following fission.

Table 12. Summary of fission experiments for decay heat analysis at very short cooling time [28].

Nuclide	Experimental method	Measurement laboratory (facility)	Year	Cooling time range (s)
	g, b spectroscopy	ORNL (Oak Ridge Research Reactor)	1980	2 – 14,000
^{235}U	calorimetry	Karlsruhe (research reactor)	1981	15 – 4,000
	g, b spectroscopy	Tokyo University (YAYOI fast research reactor)	1982	10 – 20,000
	g, b spectroscopy	Uppsala University/Studsvik (Van de Graff)	1987	10 – 10,000
	g, b spectroscopy	University of Massachusetts, Lowell (Van de Graff)	1997	0.2 – 40,000
	g, b spectroscopy	Tokyo University (YAYOI fast research reactor)	1982	10 – 20,000
^{238}U	g, b spectroscopy	University of Massachusetts, Lowell (research reactor)	1997	0.4 – 40,000
^{233}U	g, b spectroscopy	Tokyo University (YAYOI fast research reactor)	1982	10 – 20,000
^{239}Pu	g, b spectroscopy	ORNL (Oak Ridge Research Reactor)	1980	$2 – 14\times10^3$
	g, b spectroscopy	Tokyo University (YAYOI fast research reactor)	1982	10 – 20,000
	g, b spectroscopy	University of Massachusetts, Lowell (Van de Graff)	1997	0.2 – 40,000
^{241}Pu	g, b spectroscopy	ORNL (Oak Ridge Research Reactor)	1980	$2 – 14\times10^3$
^{232}Th	g, b spectroscopy	Tokyo University (YAYOI fast research reactor)	1982	10 – 20,000

4.2.2 Models

Decay heat calculations were performed with ORIGEN for each fission benchmark listed in Table 12 by assuming a very short irradiation time at a high flux of the nuclide, followed by decay over a cooling time as applicable to the considered experiment. The decay heat results obtained in W were converted to the energy release rate per fission (MeV/s per fission) and were then multiplied by the cooling time (s) to obtain the units of MeV/fission. This ensured consistency with the units reported by the experimental studies.

The results for these types of simulations strongly depend on the fission yield data (especially for the very short-lived fission products that decay away in seconds), the decay schemes, and the recoverable energy per decay used with ORIGEN. The decay data resource (including decay schemes and energy release per fission) in SCALE 6.2.4 is based on ENDF/B-VII.1 evaluations [1]. The fission yield resource (independent fission product yields) is based on ENDF/B-VII.0, with revised data being adopted for ^{235}U(thermal), ^{238}U(fast), and ^{241}Pu(thermal) independent fission yields to address inconsistencies between the direct and cumulative fission yields in ENDF/B-VII.0 [1].

4.2.3 Results

The comparison of the calculated and measured decay heat is illustrated in Figures 24–27. The plots show the energy release in MeV/fission as function of cooling time. The error bars shown for the measured data points correspond to the reported measurement uncertainties (1σ). The ORIGEN calculated values are displayed using a continuous line. The results obtained herein are similar to those from previous calculations that were performed with ORIGEN using decay data and fission yields based on ENDF/B-VI [28].

The results for the energy release following ^{235}U fission that are presented in Figure 23 show generally good agreement between calculated and measured values, within the level of the reported measurement uncertainties. For a better illustration of the details and given the differences in the experimental method used and the cooling time range covered, the results corresponding to the Karlsruhe experiments

(calorimetry) are shown separately from those for the ORNL, YAYOY, and Lowell experiments (γ, β spectroscopy). The 200 s irradiation time for the Karlsruhe samples was also significantly greater than for the other experiments. The left plot in Figure 23 shows the results for the energy release following ^{235}U thermal fission (ORNL and Lowell experiments) and the energy release following ^{235}U fast fission (YAYOY experiments) for convenience, and given that the difference between the energy release from ^{235}U fission induced by thermal neutrons was estimated to be within 1% of that induced by fast neutrons [28]. As shown in Figure 23, the calculation clearly overestimates the Lowell measurement values at cooling times above 3,000 s; as stated in Gauld et al. 2010 [28], this discrepancy is likely due to approximations used when reporting measurement values to account for the effect of noble gas loss, which is more important at longer than at shorter cooling times.

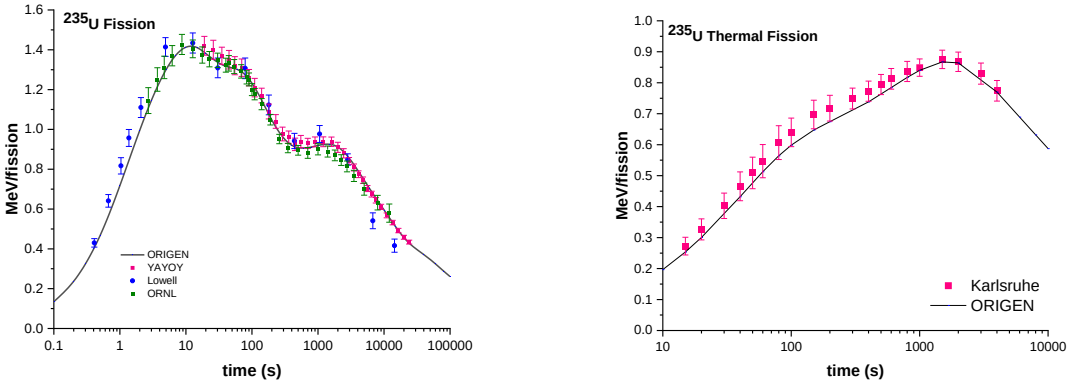

Figure 23. Decay heat calculation-experiment comparison for ^{235}U thermal fission.

The comparison experiment-calculation for the energy release following ^{239}Pu fission and ^{241}Pu thermal fission are displayed in Figure 24, and they show an agreement between calculated and measured values that is generally within the reported experimental uncertainties. As also noted for ^{235}U fission, the Lowell experimental data for ^{239}Pu fission at longer cooling times are significantly lower than those for the calculated data. The plot for the energy release following ^{239}Pu fission includes data from experiments performed with a thermal neutron spectrum (ORNL and Lowell) and a fast neutron spectrum (YAYOY). The ^{239}Pu energy release from thermal fission is less than 1% different from that released in a fast fission [28].

The calculation-experiment comparison for ^{233}U and ^{232}Th fast fission is shown in Figure 25 and is based on YAYOY experimental data. The calculation-experiment comparison for ^{238}U fast fission is shown in Figure 26 and is based on both YAYOY and Lowell measurements. The agreement between measurement and calculation is generally within the 1σ measurement uncertainty. For ^{232}Th fast fission, the calculation underestimates the experiment data for cooling times under 100s, and it is within 2σ measurement uncertainty for ~5,000–10,000 s cooling times.

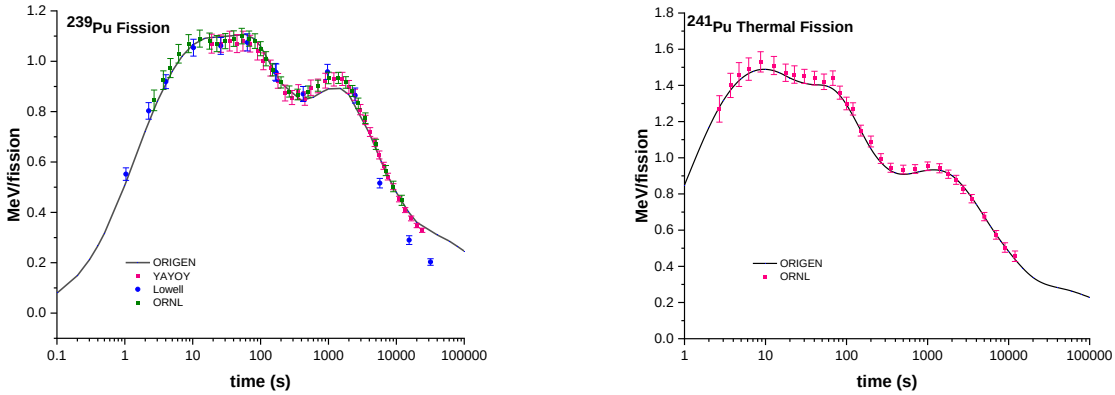

Figure 24. Decay heat calculation-experiment comparison for ^{239}Pu and ^{241}Pu thermal fission.

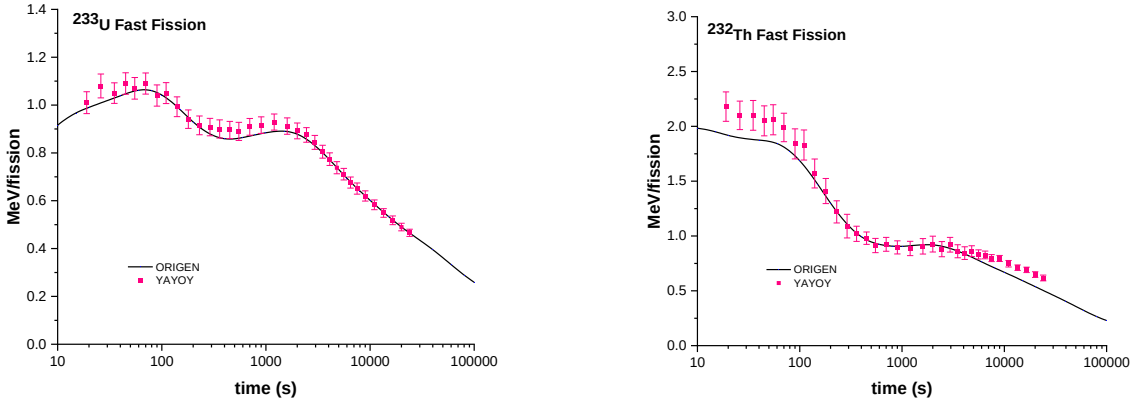

Figure 25. Decay heat calculation-experiment comparison for ^{233}U and ^{232}Th fast fission.

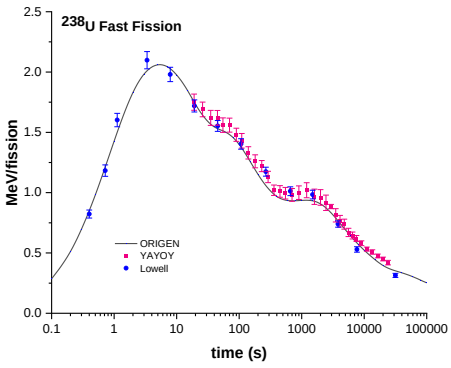

Figure 26. Decay heat calculation-experiment comparison for ^{238}U fast fission.

4.3 DISCUSSION

Validation for decay heat at cooling times of relevance to transportation, storage, and disposal of spent fuel was performed based on 91 PWR and 145 BWR full-assembly decay heat measurements. These measurements cover a cooling time ranging from 2 to 27 years for PWRs and BWRs, a burnup range of 18–51 GWd/MTU for PWRs, and a burnup range of 5–45 GWd/MTU for BWRs. The comparison calculation-experiment shows good agreement. The histograms of the C/E data are presented in Figure 27. The mean C/E values are 1.006 (σ=0.016) for PWRs and 0.984 (σ=0.077) for BWRs.

The C/E results obtained with SCALE 6.2.4/ENDF/B-VII.1 and those obtained with SCALE 6.1/ENDF/B-VII.0 when using a consistent validation basis (see Table 13) differ on average by 0.6% (σ=0.5%) for PWR assemblies and by 1.2% (σ=0.8%) for BWR assemblies. This difference was found to be primarily due to the change in ^{238}Pu capture cross section between ENDF/B-VII.0 and ENDF/B-VII.1 [46]. The prediction of the ^{238}Pu in PWR spent fuel, as noted in Section 3.2.3, significantly improved by ~8% with SCALE 6.2.4/ENDF/B-VII.1 compared to SCALE 6.1/ENDF/B-VII.0.

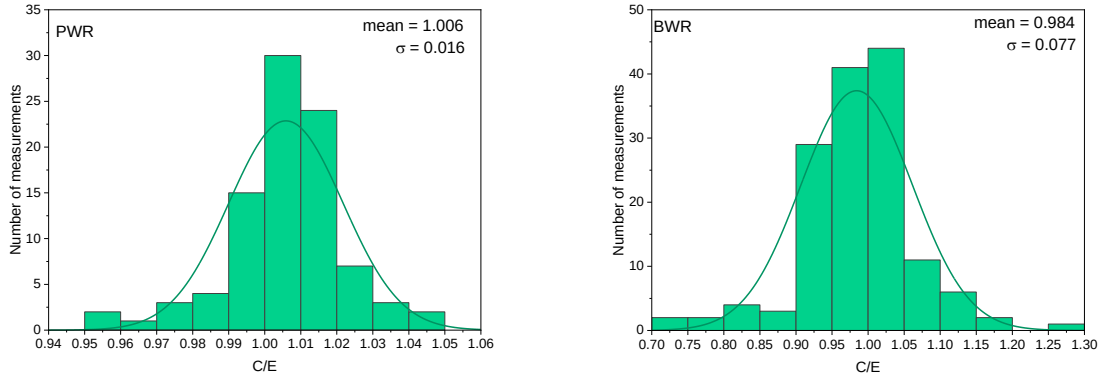

Figure 27. Histogram plots for decay heat calculation-experiment comparison.

Table 13. Decay heat comparison between SCALE 6.2.4/ENDF/B-VII.1 and SCALE 6.1/ENDF/B-VII.0.

Reactor name	Reactor type	No. of measurements	Cooling time (year)	C/E SCALE 6.2.4 ENDF/B-VII.1		C/E SCALE 6.1 ENDF/B-VII.0		C/E (VII.1) – C/E (VII.0)	
				mean	σ	mean	σ	mean	σ
Ringhals 2	PWR	33	15.9 – 26.7	1.006	0.013	0.998	0.012	0.008	0.003
Ringhals 3	PWR	38	12.9 – 25.9	1.009	0.012	1.005	0.011	0.004	0.006
Ringhals 1	BWR	45	12.6 – 23.6	1.009	0.025	0.999	0.024	0.010	0.002
Oskarshamn 2	BWR	5	20.3 – 26.7	1.010	0.024	0.975	0.020	0.036	0.007
PWR		71	15.9 – 25.9	1.008	0.012	1.013	0.013	0.006	0.005
BWR		50	12.6 – 26.7	1.009	0.024	1.002	0.012	0.012	0.008
PWR+BWR		121	12.6 – 26.7	1.008	0.018	1.000	0.017	0.009	0.007

Assessments of the impact of experimental uncertainties on the C/E comparisons and the effect of uncertainties in modeling input data or nuclear data on the calculated decay heat are included in previous publications [31, 48, 49].

5. FULL-CORE ANALYSIS

Full-core LWR analyses with SCALE for the WBN1 PWR provided CE reference solutions for verification of MG analyses performed with the VERA core simulator [36, 37]. SCALE models that were previously developed for this reactor served as a basis for the recent analysis with SCALE 6.2.4 and ENDF/B-VII.1 nuclear data of the core configuration presented here. This section also presents validation results for two non-LWR reactors that were analyzed with previous SCALE versions and associated nuclear data [32-34].

5.1 PWR FULL-CORE VALIDATION EXAMPLE

5.1.1 Watts Bar 1

Watts Bar Nuclear Unit 1 (WBN1) is a Westinghouse four-loop PWR operated by the Tennessee Valley Authority (TVA). It started operation at 3,411 MWth power in 1996. The reactor has 193 fuel assemblies of a Westinghouse 17×17 lattice design that are contained in a cylindrical core. Each assembly includes 264 fuel rods and 25 guide and instrument tubes. The core layout and one of the assembly configurations [36, 37] are illustrated in Figure 28. The startup physics testing for WBN1 has provided valuable benchmarking data that have been made publicly available by TVA, contributing to the extensive validation basis developed for the Consortium for Advanced Simulation of Light Water Reactors (CASL) VERA core simulator [36, 37].

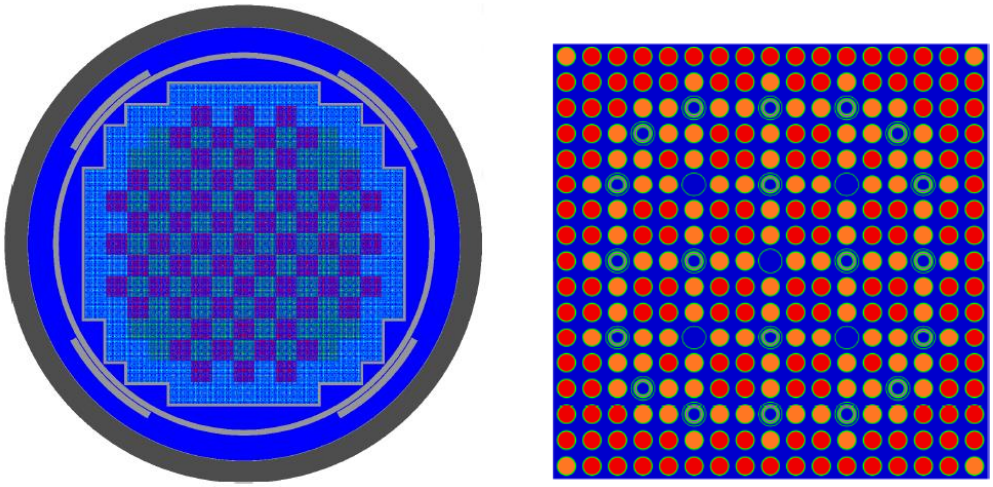

Figure 28. WBN1 core layout and sample assembly lattice [36, 37].

5.1.1.1 Experimental data

The experimental data used in the current study were obtained from the publicly available WBN1 Cycle 1 zero power physics test data, along with a detailed core configuration and operating history, including a critical boron history of the first 12 cycles. These startup tests were performed at hot-zero-power isothermal conditions of ~565 K and 2,250 psi, and the coolant critical soluble boron concentration varied between 1,177 and 1,299 ppm. The experimental data considered in the current report include initial criticality and differential boron reactivity worth.

The Cycle 1 core loading used three UO_2 enrichment regions (2.11, 2.619, and 3.10% ^{235}U), discrete annular borosilicate glass (Pyrex) burnable absorber rods, and hybrid B_4C control rods with Ag-In-Cd tips. The assembly enrichment map within the core and control rod bank positions are illustrated in Figure

29. Initial criticality was achieved by diluting the boron in the reactor coolant system and positioning the regulating control bank, Bank D. Detailed descriptions of these validation data are available in the literature [36, 37].

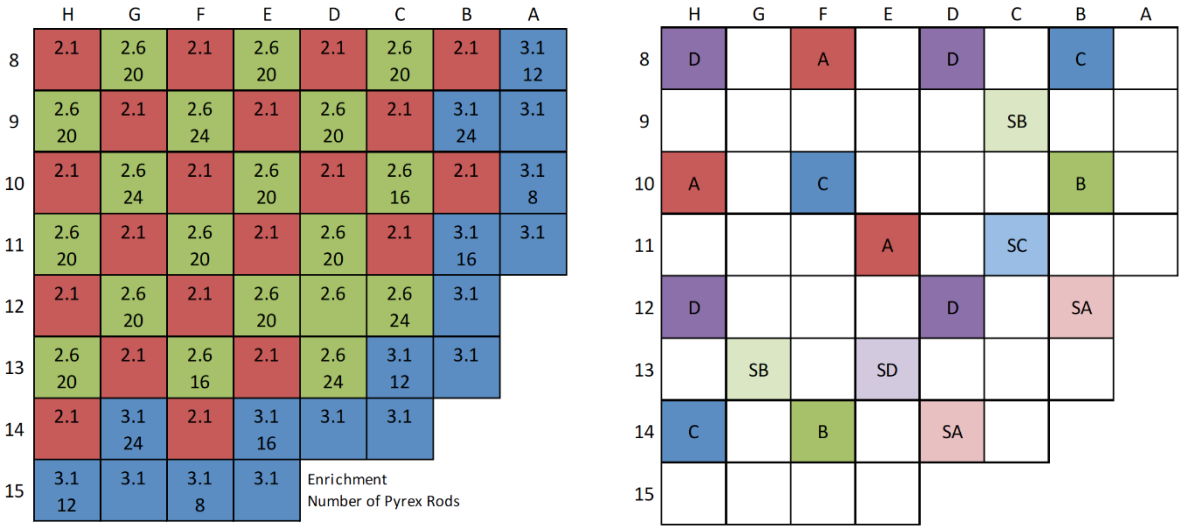

Figure 29. WBN1 Cycle 1 assembly enrichments and control rod bank positions [36, 37].

5.1.1.2 Models

The simulations performed for the current study are based on the previously developed full-core 3D model [36] that was developed with the KENO-VI Monte Carlo neutron transport code in SCALE, in which most core's features are modeled explicitly, whereas the regions above and below the fuel rods are treated as homogenized regions. The input file of this 3D KENO-VI model includes nine million ASCII input lines and 800,000 unique geometry units. The model is illustrated in Figure 30, and modeling details are available in publications by Godfrey et al. [36, 37].

The 3-D model was used with SCALE 6.2.4 and CE ENDF/B-VII.1 cross sections to calculate the eigenvalue for the startup core and the differential boron reactivity, for comparison to corresponding measurement data. The differential boron reactivity worth was determined based on modeling a single 120 ppm boron perturbation in the coolant. The computational resources are significant, given the high complexity of the configuration. The eigenvalue simulation targeting a statistical uncertainty of the order of pcm in the Monte Carlo neutron transport simulation required 7.5×10^9 neutron histories and took 41 hours and 120 processors to complete.

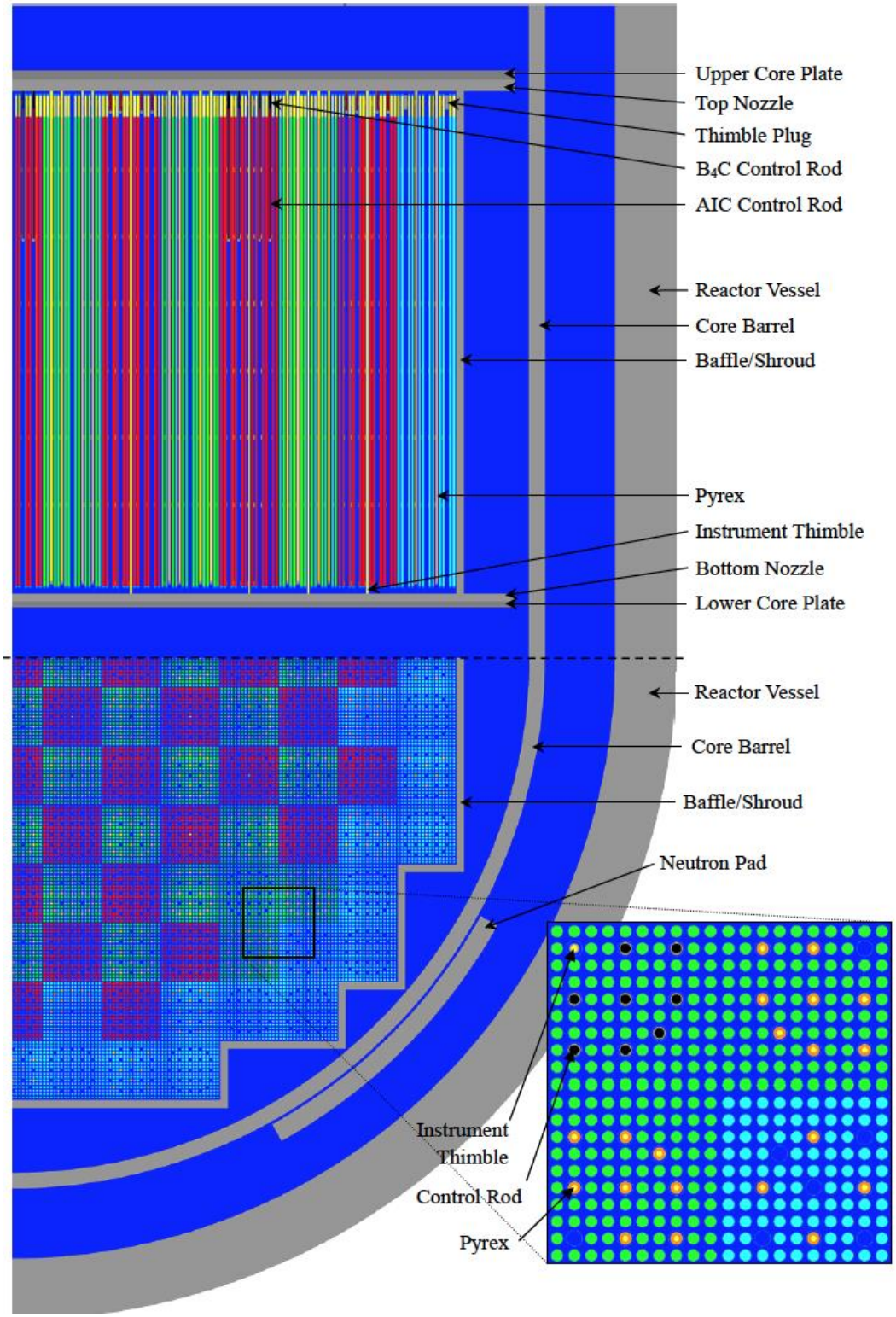

Figure 30. WBN1 KENO-VI model [36].

5.1.1.3 Results

A comparison of measurement and calculation results is presented in Table 14 for initial eigenvalue and differential boron worth.

Table 14. WBN1 Cycle 1 results.

Metric	Measured	SCALE 6.2.4 ENDF/B-VII.1	Difference
Initial eigenvalue	1.00000	0.999513 ± 0.000011	49 pcm
Differential boron worth (pcm/ppm)	10.77	10.21	-5.2 %

5.2 NON-LWR

As part of an NRC-funded project to quantify severe accident source terms for non-LWRs, ORNL is using SCALE to model and evaluate several advanced reactor systems based on information provided in open literature. Once these models are finalized and documented, they will become part of the SCALE validation basis. In the following sections, results are provided for two high-temperature gas cooled reactors (HTGRs) for which SCALE models were previously developed and documented [32–34].

5.2.1 HTR-10

The HTR-10 is a small (1.8 m diameter × 1.97 m mean height), helium-cooled, graphite moderated, 10MWth prototype pebble-bed HTGR operated in China. The fuel element for this reactor (fuel pebble) is a 3 cm radius sphere that contains a 2.5 cm radius inner zone with thousands of 0.455 mm radius tristructural isotropic (TRISO) fuel particles randomly distributed in a graphite matrix. The pebble's inner zone is covered by a 0.5 cm thick graphite shell. Each TRISO fuel particle contains UO_2 fuel kernels with 17% ^{235}U enrichment that are surrounded with multiple silicon carbide and graphite layers. The HTR-10's first critical core contained ~17,000 fuel pebbles, as well as dummy (unfueled) graphite pebbles with a fuel-to-dummy pebble ratio of approximately 57:43. An evaluated benchmark is available for the HTR-10's initial critical core in the International Reactor Physics Experiment Evaluation (IRPhE) Handbook [50].

5.2.1.1 Experimental data

The IRPhE HTR-10 benchmark is based on the first critical core experiment that was performed in the year 2000 with fresh fuel and at room temperature. Criticality was achieved with control rods withdrawn. The IRPhE benchmark provides detailed model specifications for this initial critical core, as well as the experimental eigenvalue and corresponding experimental uncertainty. Two sets of benchmark specifications are provided, with the only difference between the two being the level of detail for specifying the structures in the reflector region. The benchmark dataset considered in this report is the so-called High-Fidelity Model. In this model, the 20 coolant flow channels, 13 control rod channels, 7 small absorber ball channels, and one hot gas duct are explicitly represented in the reflector region.

5.2.1.2 Models

Full 3D models for the HTR-10 have been developed using the KENO-VI Monte Carlo neutron transport code and are discussed in detail by Ilas et al. [33]. The reactor has a cylindrical active core region located above a conical pebble discharge tube and a cylindrical discharge tube. For the initial critical configuration, there were 16,890 fuel and moderator pebbles in the active core region (9,627 fuel pebbles and 7,263 moderator pebbles), for a 57:43 fuel-to-moderator pebble ratio. The conical and cylindrical discharge tubes beneath the active core region were filled with moderator pebbles only, with a

packing fraction of 61%. The reflector region surrounding the active core region and the discharge tubes are zones with varying material densities of carbon, natural boron, and coolant components.

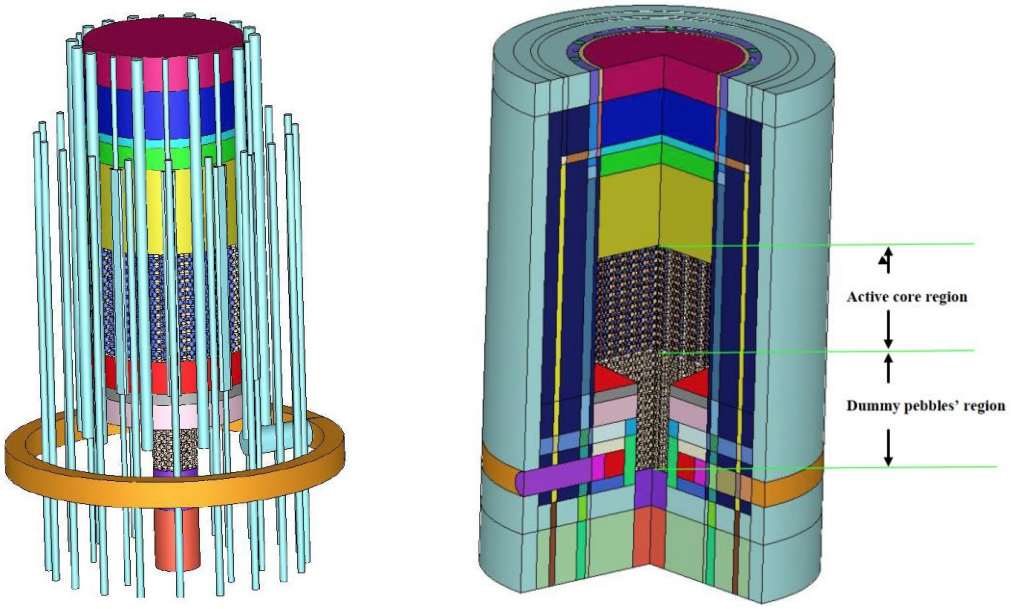

Figure 31. Illustration of HTR-10 benchmark model details (channels in reflector regions [left], full reactor model [right]; images not to scale) [33].

The two SCALE models available for this HTR-10 high-fidelity benchmark were used for simulations. One is a CE model in which the fuel pebbles and the fuel kernels within a pebble are individually modeled, with ENDF/B-VII.1 CE cross sections used for simulations. The other is an MG model in which the fuel kernels within a fuel pebble are not individually modeled; however, the double heterogeneity is accounted for by using the *doublehet* cross section processing option in SCALE. The calculations for the MG model used the 252-group ENDF/B-VII.1 cross section library. The criticality source in each of these two CE and MG models was defined with 10^5 neutrons per generation, 1100 generations, and 100 generations skipped.

5.2.1.3 Results

Comparison of the calculated eigenvalue and the benchmark-provided value for the HTR-10 initial critical state is presented in Table 15. The uncertainty in the benchmark eigenvalue is specified in the IRPhE Handbook as an overall uncertainty accounting for experimental uncertainties in the modeling parameters. The uncertainties in the calculated eigenvalues represent statistical uncertainties in the Monte Carlo neutron transport simulations with KENO-VI. The difference between the KENO-calculated CE and MG eigenvalues is small at 107 pcm (σ=13 pcm), demonstrating that the *doublehet* treatment is a good approximation for this type of configuration.

The difference between the calculated and benchmark eigenvalue is 271 pcm for the CE model and 378 pcm for the MG model. For both CE and MG models, the calculated value agrees well with the experiment value, being approximately within the reported experimental uncertainty of 370 pcm.

Table 15. Eigenvalue results for high-fidelity HTR-10 benchmark.

	k-eff	σ	Δ k-eff[a] (pcm)
Benchmark value [50]	1.0000	0.0037	reference
SCALE/KENO-VI MG	1.00378	0.00008	378 ± 370
SCALE/KENO-VI CE	1.00271	0.00010	271 ± 370

[a] calculated as 10^5(k-eff$_{calculated}$ – k-eff$_{benchmark}$).

5.2.2 HTTR

The HTTR is a helium-cooled, graphite moderated, 30 MWth prismatic core HTGR operated in Japan. The fuel element for this reactor is an annular fuel rod with a 0.5 cm inner radius and a 1.3 cm outer radius, with each fuel rod including ~ 3,000 TRISO fuel particles embedded in a graphite matrix. Each fuel rod is enclosed in a graphite sleeve, with helium circulating outside this sleeve. Each TRISO fuel particle has a 0.46 cm radius and contains a UO_2 fuel kernel that is surrounded with multiple silicon carbide and graphite layers; the fuel enrichments vary between 3.3 and 9.9% ^{235}U. The HTTR fuel assembly is a hexagonal prism 58 cm in height with a flat width of 36 cm. Each fuel assembly contains either 31 or 33 annular fuel rods. The fuel assemblies are stacked on top of each other, forming fuel columns with an active height of 290 cm. The configurations of the fuel rods and fuel block are illustrated in Figure 32 [51]. The fully loaded HTTR core had 30 fuel columns, intermixed with control rods blocks, and surrounded by reflector blocks.

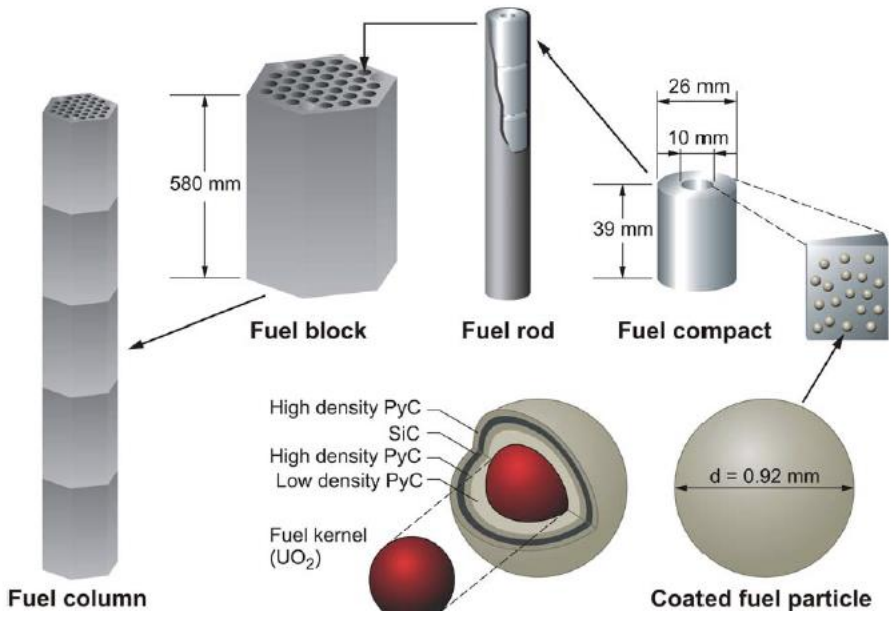

Figure 32. Illustration of HTTR fuel block components [51].

The cross-sectional view of this core in Figure 33 shows four fuel blocks zones labeled 1 through 4; control rods blocks (one central [C] and the others placed in rings R1 through R4); instrumentation columns (I); and replaceable reflector columns (RR).

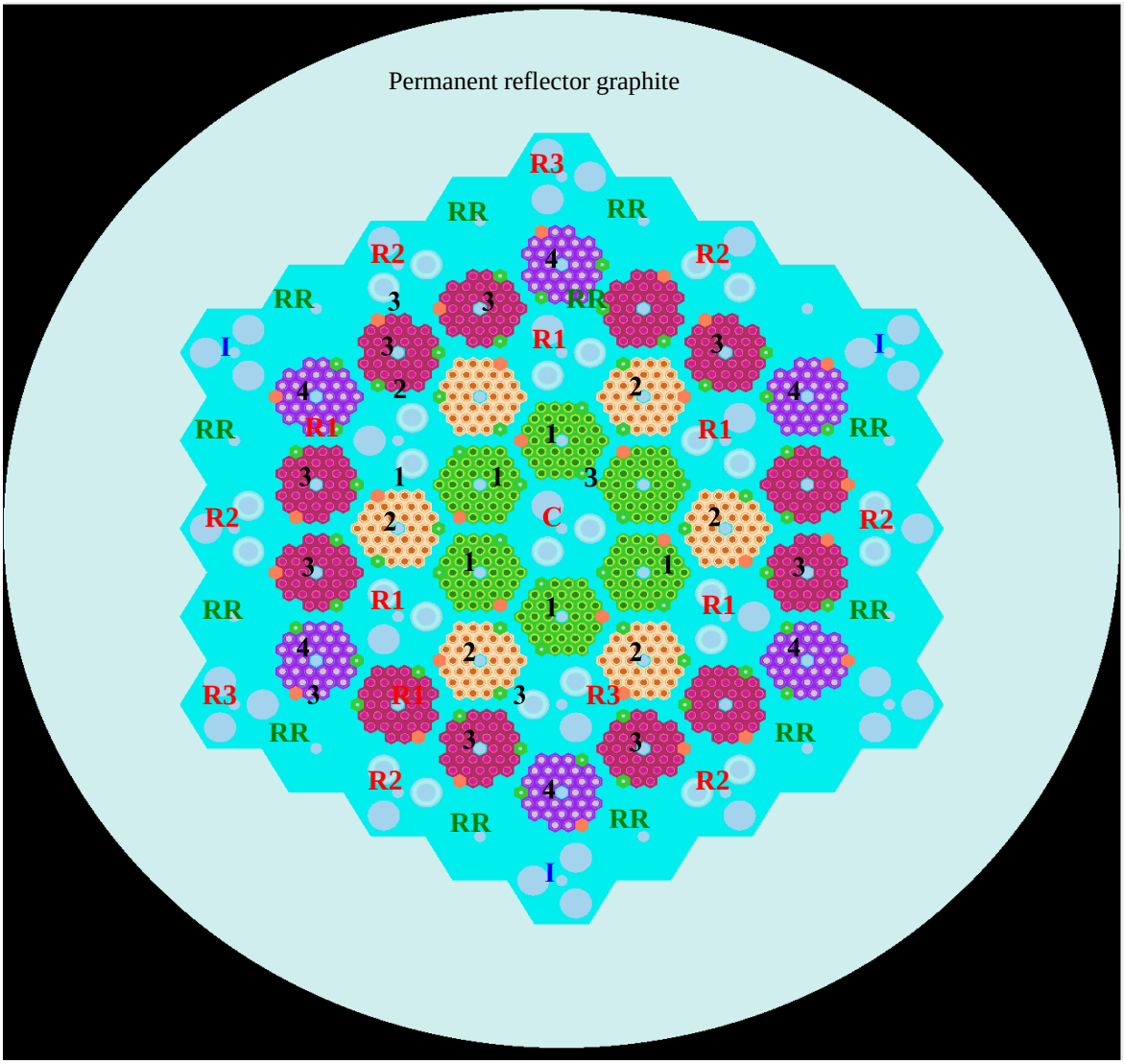

Figure 33. Illustration of HTTR fully loaded core benchmark model: cross sectional view [33].

5.2.2.1 Experimental data

The IRPhE Handbook contains several benchmarks for subcritical and critical HTTR configurations. The first fully loaded core criticality [51] was achieved in December 1998. The configuration of the core at full power is the same as that of the fully loaded initial core. The benchmark considered here is the fully loaded initial HTTR critical core with 30 fuel columns. This benchmark is based on one of the initial isothermal critical core tests. The power in these tests was limited to 30 W, and the temperature was limited to 950°C. The reported experimental eigenvalue for this benchmark is 1.0025, with an evaluated uncertainty between -0.0060 and +0.0071.

5.2.2.2 Models

SCALE 3D CE and MG models of the HTTR fully loaded initial critical core benchmark were previously developed and used in SCALE 6.1 validation studies. In the CE model, the fuel rods and the fuel kernels in the rods are individually modeled. In the MG model, the double heterogeneity is accounted for by using the *doublehet* cross section processing option in SCALE. In the first developed MG model for

HTTR [33, 34], developed using SCALE 6.1, since the *doublehet* processing methodology as implemented in SCALE at the time did not allow the use of annular fuel rods, the HTTR annular fuel rod was approximated as a cylindrical fuel rod by combining the inner helium region with the graphite matrix. This MG model was slightly revised later [35] to take advantage of the new annular *doublehet* rod capability implemented in SCALE 6.2.

The calculations for the MG models in this study used the 252-group ENDF/B-VII.1 cross section library, and the CE model simulations used CE ENDF/B-VII.1 nuclear data. The criticality source in each of these two models was defined with 10^5 neutrons per generation, 1100 generations, and 100 generations skipped.

5.2.2.3 Results

Comparison of the calculated and benchmark eigenvalues for the HTTR's initial critical fully loaded core is presented in Table 16. The uncertainty in the benchmark eigenvalue was specified in the IRPhE Handbook [51] as an overall uncertainty accounting for experimental uncertainties in the modeling parameters. The uncertainties in the calculated eigenvalues represent statistical uncertainties in the Monte Carlo neutron transport simulations. Results are shown for both MG models' (annular fuel rod; cylindrical fuel rod) *doublehet* approaches.

The results of the CE and MG models with annular *doublehet* are practically the same. The comparison of the results for the two MG model variants shows an impact of the approximation used within the *doublehet* option for the fuel rod of less than 100 pcm. The difference between the CE-calculated and benchmark eigenvalues is 505 pcm. Although the difference is large, this is a significant improvement compared to the corresponding difference between the SCALE 6.1 with ENDF/B-VII.0 CE data and the benchmark value, which was ~1,600 pcm. As noted by Bostelmann et al. [35], most of this difference is due to the change in the carbon capture cross section between ENDF/B-VII.0 and ENDF/B-VII.1, with a high impact on graphite-rich systems like HTTR.

Table 16. Eigenvalue results for fully loaded HTTR benchmark.

	k-eff	σ	Δ k-eff[b] (pcm)
Benchmark value [51]	1.0025	-0.0060, +0.0071	reference
SCALE6.2.4/KENO-VI CE	1.00755	0.00010	505 (-61,+72)
SCALE6.2.4/KENO-VI MG (annular DH[a])	1.00760	0.00008	510 (-60,+71)
SCALE6.2.4/KENO-VI MG (cylindrical DH)	1.00679	0.00007	429 (-60,+71)

[a] DH = doublehet; [b] calculated as $10^5(\text{k-eff}_{\text{calculated}} - \text{k-eff}_{\text{benchmark}})$

5.3 DISCUSSION

Validation examples are shown for full-core analysis with SCALE 6.2.4 and ENDF/B-VII.1 data for both LWR and non-LWR configurations. While SCALE does not have a core simulator for LWR to enable computationally efficient full-core analyses, it can serve, as demonstrated here and in other previous publications [36, 37] for developing CE reference solutions for specific reactor state points. The LWR validation examples considered here are based on startup experiments for WBN1, and they show good agreement between calculation and measurement results. The calculated eigenvalue is consistent with that from the experiment (49 pcm difference), and the predicted differential boron worth is within 5% of the measurement.

Validation examples for non-LWRs include two HTGRs: a pebble bed design and a prismatic core design. CE and MG models have been used to model the HTR-10 [50] and HTTR [51] initial critical core benchmarks available from the IRPhE Handbook, with a reasonable agreement being observed between

the calculated and benchmark eigenvalues. For the HTR-10 benchmark, the calculated eigenvalues for both CE and MG models agree with the benchmark value within the experimental uncertainty. In the case of the HTTR benchmark, the calculation overestimates the experiment by ~500 pcm; however, this is a significant improvement on the order of 1,000 pcm from previous results obtained with SCALE 6.1 and ENDF/B-VII.0 libraries.

Notably, the CE and MG calculated values are in good agreement for a given HTGR configuration, demonstrating the good performance of the *doublehet* capability available in SCALE for MG simulations of double heterogeneous fuel systems. The value of this capability will be even more important in depletion simulations, in which the use of a CE neutron transport solver is computationally intensive and likely impractical for complex HTGR systems. Such systems target burnups of over 100 GWd/MTU and would require a significant number of depletion steps in the simulation.

6. CONCLUSION

Quantifying and evaluating the bias in the prediction of key metrics of interest to reactor physics applications—such as eigenvalue, nuclide inventory, and decay heat—is essential for understanding the performance of capabilities and associated nuclear data in SCALE 6.2.4 and their adequacy for lattice and full-core physics safety-related analyses. The impact goes well beyond reactor physics and the back-end of fuel cycle to support modeling challenges in other areas, such as isotope production, national security, and nonproliferation applications, for which adequately simulating nuclide transmutations and decay in nuclear fuel during and post irradiation is of great importance.

This report summarizes validation studies to quantify the bias in calculated nuclides inventories and decay heat for LWR nuclear fuel, and eigenvalue for selected LWR and HTGR full cores, as determined with SCALE 6.2.4 and ENDF/B-VII.1 nuclear data. The experimental validation basis includes 92 PWR and 76 BWR spent fuel samples measurements, 91 PWR and 145 BWR full-assembly decay heat measurements, fission experiments for decay heat measurements at very short cooling time in six types of fissile nuclides, and initial critical core eigenvalue measurements for one LWR and two non-LWR full cores. The considered experiments are modeled using different capabilities in SCALE 6.2.4 (TRITON depletion sequence, Polaris lattice physics code, and KENO-VI Monte Carlo neutron transport code). The measured metrics are compared to the corresponding calculated values. The bias calculated with SCALE 6.2.4/ ENDF/B-VII.1 is compared with that obtained with SCALE 6.1 and ENDF/B-VII.0 data for the cases for which previous validation results are available.

The comparison of calculation vs. experiment results shows good agreement on average, considering the uncertainties associated with the experimental data, for many of the 40 measured nuclides of importance to burnup credit, decay heat, and radiation shielding applications. The two major actinides are well predicted on average: for ^{235}U in PWR and BWR, within 1% (σ=4%) and 3% (σ=11%) of the experiment, respectively, and for ^{239}Pu in PWR and BWR, within 2% (σ=3%) and 3% (σ=8%) of the measurement, respectively. Compared to corresponding SCALE 6.1/ ENDF/B-VII.0 validation, a notable improvement is observed in the calculated ^{238}Pu and ^{239}Pu actinides, for which the prediction for PWR fuel improves on average by ~8% (σ=9%) and ~2% (σ=5%), respectively.

The comparison of calculation vs. experiment results for full-assembly decay heat at cooling times of relevance to transportation, storage, and disposal of spent fuel shows good agreement. The bias in assembly decay heat is on average less than 1% (σ=2%) for PWR and less than 2% (σ=8%) for BWR for the analyzed assembly experiments. Compared to corresponding SCALE 6.1/ ENDF/B-VII.0 validation, the decay heat's calculated bias does not change significantly, the change being on average ~1% (σ=1%) for both PWR and BWR results. The results for the fissile material experiments at cooling times up to ~10^5 s, as relevant to loss-of-coolant accident scenarios, show generally good agreement between calculated and measured values of energy release following fission for ^{233}U, ^{235}U, ^{238}U, ^{239}Pu, ^{241}Pu, and ^{232}Th thermal and/or fast fission. The comparison in this case is similar to that observed with previous SCALE and associated nuclear data libraries versions.

The validation examples for full-core eigenvalue show good agreement between calculated and measured eigenvalues for the considered LWR (WBN1) and HTGR (HTR-10 and HTTR) initial critical core experiments. The eigenvalue bias is less than 50 pcm for WBN1, within the benchmark experiment uncertainty (370 pcm) for HTR-10, and within ~500 pcm of criticality for HTTR. The results obtained indicate adequate applicability of the unique *doublehet* capability available in SCALE for the analysis of HTGR configurations, based on the analysis of the considered pebble bed and prismatic systems, with a very good agreement between the CE and MG calculated eigenvalues. Compared to previous validation performed with SCALE 6.1/ENDF/B-VII.0, the results obtained with SCALE 6.2.4/ENDF/B-VII.1 are consistent for the WBN1 benchmark, whereas for the two HTGRs' benchmarks, the significant update in

ENDF/B-VII.1 data compared to ENDF/B-VII.0 data for carbon capture cross section leads to an improvement of over 1,000 pcm in calculated bias.

Quantifying and evaluating the bias and uncertainty in code predictions of key metrics associated with fuel depletion, such as spent nuclear fuel compositions, is necessary to validate the accuracy of the codes and nuclear data used for reactor safety and licensing calculations. Determination of this bias and uncertainty is a continuous process, as these values must be reassessed to keep pace with changes in the fuel characteristics for fuel currently used or planned for commercial reactors in the future. The modern fuels are characterized by higher burnups, higher enrichments, complex and heterogeneous assembly designs, and improved reactor operation. Moreover, the bias and uncertainty values must be updated to account for changes in the computational capabilities and evaluated nuclear data that are used for simulations. The validation examples provided in this report for SCALE 6.2.4/ENDF/B-VII.1 will be reassessed with SCALE 6.3/ENDF/B-VIII.0 and will be documented in the next SCALE 6.3 validation report. The experimental data used as validation basis will be expanded to include additional measurements or computational models as they become available.

7. REFERENCES

1. Wieselquist W.A., Lefebvre R.A., Jessee M.A., eds, *SCALE Code System*, 2020. ORNL/TM-2005/39, V.6.2.4., https://www.ornl.gov/file/scale-62-manual/display
2. Chadwick, M.B., M. Herman, P. Obložinský, M.E. Dunn, Y. Danon, A.C. Kahler, D.L. Smith, B. Pritychenko, G. Arbanas, R. Arcilla, R. Brewer, D.A. Brown, R. Capote, A.D. Carlson, Y.S. Cho, H. Derrien, K. Guber, G.M. Hale, S. Hoblit, S. Holloway, T.D. Johnson, T. Kawano, B.C. Kiedrowski, H. Kim, S. Kunieda, N.M. Larson, L. Leal, J.P. Lestone, R.C. Little, E.A. McCutchan, R.E. MacFarlane, M. MacInnes, C.M. Mattoon, R.D. McKnight, S.F. Mughabghab, G.P.A. Nobre, G. Palmiotti, A. Palumbo, M.T. Pigni, V.G. Pronyaev, R.O. Sayer, A.A. Sonzogni, N.C. Summers, P. Talou, I.J. Thompson, A. Trkov, R.L. Vogt, S.C. van der Marck, A. Wallner, M.C. White, D. Wiarda, and P.G. Young, "ENDF/B-VII.1 Nuclear Data for Science and Technology: Cross Sections, Covariances, Fission Product Yields and Decay Data." *Nuclear Data Sheets*, 2011. 112(12): p. 2887. https://www.sciencedirect.com/science/article/pii/S009037521100113X
3. Vaccaro, S., I.C. Gauld, J. Hu, P. De Baere, J. Peterson, P. Schwalbach, A. Smejkal, A. Tomanin, A. Sjöland, S. Tobin, and D. Wiarda, "Advancing the Fork Detector for Quantitative Spent Nuclear Fuel Verification." *Nuclear Instruments and Methods in Physics Research. Section A, Accelerators, Spectrometers, Detectors and Associated Equipment*, 2018: p. 202. https://www.osti.gov/servlets/purl/1424458
4. Hu, J., I.C. Gauld, S. Vaccaro, T. Honkamaa, and G. Ilas, "Validation of ORIGEN for VVER-440 Spent Fuel with Application to Fork Detector Safeguards Measurements." *ESARDA Bulletin*, 2020: p. 28. https://www.osti.gov/servlets/purl/1649471
5. Hu, J., G. Ilas, and I.C. Gauld, *Analysis with the ORIGEN Module of PNAR Spent Fuel Measurements for Nuclear Safeguards Applications*, 2020. ORNL/TM-2020/1834, Oak Ridge National Laboratory. https://www.osti.gov/servlets/purl/1760108
6. Hermann, O.W., S.M. Bowman, C.V. Parks, and M.C. Brady, *Validation of the SCALE System for PWR Spent Fuel Isotopic Composition Analyses*, 1995. ORNL/TM-12667, Oak Ridge National Laboratory https://www.osti.gov/servlets/purl/57886
7. DeHart, M.D. and O.W. Hermann, *An Extension of the Validation of SCALE (SAS2H) Isotopic Predictions for PWR Spent Fuel*, 1996. ORNL/TM-13317, Oak Ridge National Laboratory. https://www.osti.gov/servlets/purl/405743
8. Ilas G., Gauld I.C., Difilippo F.C., Emmett M.B, *Analysis of Experimental Data for High Burnup PWR Spent Fuel Isotopic Validation – Calvert Cliffs, Takahama, and Three Mile Island Reactors*, 2010. NUREG/CR-6968, www.nrc.gov/reading-rm/doc-collections/nuregs/contract/cr6968/
9. Ilas G., Gauld I.C., Murphy B.D., *Analysis of Experimental Data for High Burnup PWR Spent Fuel Isotopic Validation – ARIANE and REBUS Programs (UO_2 fuel)*, 2010. NUREG/CR-6969, US Nuclear Regulatory Commission www.nrc.gov/reading-rm/doc-collections/nuregs/contract/cr6969/
10. Ilas G., Gauld I.C., *Analysis of Experimental Data for High Burnup PWR Spent Fuel Isotopic Validation - Vandellos II Reactor*, 2011. NUREG/CR-7013, US Nuclear Regulatory Commission www.nrc.gov/reading-rm/doc-collections/nuregs/contract/cr7013/
11. Gauld I.C., Ilas G., Radulescu G., *Uncertainties in Predicted Isotopic Compositions for High Burnup PWR Spent Nuclear Fuel*, 2011. NUREG/CR-7012, US Nuclear Regulatory Commission www.nrc.gov/reading-rm/doc-collections/nuregs/contract/cr7012/
12. Radulescu, G., I.C. Gauld, and G. Ilas, *SCALE 5.1 Predictions of PWR Spent Nuclear Fuel Isotopic Compositions*, 2010. ORNL/TM-2010/44, Oak Ridge National Laboratory. https://www.osti.gov/servlets/purl/983556

13. G. Radulescu, I.C.Gauld, G. Ilas, J.C. Wagner, *An Approach for Validating Actinide and Fission Product Burnup Credit Criticality Safety Analyses—Isotopic Composition Predictions*, 2012. NUREG/CR-7108, US Nuclear Regulatory Commission https://www.nrc.gov/reading-rm/doc-collections/nuregs/contract/cr7108/index.html#pub-info

14. Radulescu, G., I.C. Gauld, G. Ilas, and J.C. Wagner, "Approach for Validating Actinide and Fission Product Compositions for Burnup Credit Criticality Safety Analyses." *Nuclear Technology*, 2014. 188(2): p. 154. https://doi.org/10.13182/NT13-154

15. Bowman, S.M., "SCALE 6: Comprehensive Nuclear Safety Analysis Code System." *Nuclear Technology*, 2011. 174(2): p. 126. https://doi.org/10.13182/NT10-163

16. Chadwick, M.B., P. Oblozinsky, M. Herman, N.M. Greene, R.D. McKnight, D.L. Smith, P.G. Young, R.E. MacFarlane, G.M. Hale, R.C. Haight, S. Frankle, A.C. Kahler, T. Kawano, R.C. Little, D.G. Madland, P. Moller, R. Mosteller, P. Page, P. Talou, H. Trellue, M. White, W.B. Wilson, R. Arcilla, C.L. Dunford, S.F. Mughabghab, B. Pritychenko, D. Rochman, A.A. Sonzogni, C. Lubitz, T.H. Trumbull, J. Weinman, D. Brown, D.E. Cullen, D. Heinrichs, D. McNabb, H. Derrien, M. Dunn, N.M. Larson, L.C. Leal, A.D. Carlson, R.C. Block, B. Briggs, E. Cheng, H. Huria, K. Kozier, A. Courcelle, V. Pronyaev, and S. der Marck, "ENDF/B-VII.0: Next Generation Evaluated Nuclear Data Library for Nuclear Science and Technology." *Nuclear Data Sheets*, 107(12), November 12, 2006, pp. 2931-3060, 2006. https://www.osti.gov/servlets/purl/900147

17. Hu J., J.M. Giaquinto, I.C. Gauld, G. Ilas, and T.J. Keever, "Analysis of New Measurements of Calvert Cliffs Spent Fuel Samples Using SCALE 6.2." *Annals of Nuclear Energy*, 2017. 106: p. 221. https://www.sciencedirect.com/science/article/pii/S0306454917300865

18. Gauld, I.C., J.M. Giaquinto, J.S. Delashmitt, J. Hu, G. Ilas, T.J. Haverlock, and C. Romano, "Re-evaluation of Spent Nuclear Fuel Assay Data for the Three Mile Island Unit 1 Reactor and Application to Code Validation." *Annals of Nuclear Energy*, 2016. 87: p. 267. https://doi.org/10.1016/j.anucene.2015.08.026

19. Ilas, G., I.C. Gauld, and G. Radulescu, "Validation of New Depletion Capabilities and ENDF/B-VII Data Libraries in SCALE." *Annals of Nuclear Energy*, 2012. 46: p. 43. https://doi.org/10.1016/j.anucene.2012.03.012

20. Hermann, O.W. and M.D. DeHart, *Validation of SCALE (SAS2H) Isotopic Predictions for BWR Spent Fuel*, 1998. ORNL/TM-13315, Oak Ridge National Laboratory https://www.osti.gov/servlets/purl/304103

21. Mertyurek, U., M.W. Francis, and I.C. Gauld, *SCALE 5 Analysis of BWR Spent Nuclear Fuel Isotopic Compositions Safety Studies*, 2011. ORNL/TM-2010/286, Oak Ridge National Laboratory https://www.osti.gov/servlets/purl/1081684

22. Gauld, I.C. and U. Mertyurek, "Validation of BWR Spent Nuclear Fuel Isotopic Predictions with Applications to Burnup Credit." *Nuclear Engineering and Design*, 2019. 345: p. 110. https://doi.org/10.1016/j.nucengdes.2019.01.026

23. Gauld, I.C., Mertyurek, U., *Margins for Uncertainty in the Predicted Spent Fuel Isotopic Inventories for BWR Burnup Credit*, 2016. NUREG/CR-7251, US Nuclear Regulatory Commission https://www.nrc.gov/reading-rm/doc-collections/nuregs/contract/cr7251/

24. Mertyurek, U. and I.C. Gauld, "Development of ORIGEN Libraries for Mixed Oxide (MOX) Fuel Assembly Designs." *Nuclear Engineering and Design*, 2015. https://www.osti.gov/servlets/purl/1286852

25. Mertyurek, U., M.A. Jessee, and B.R. Betzler, "Lattice Physics Calculations Using the Embedded Self-Shielding Method in Polaris, Part II: Benchmark Assessment." *Annals of Nuclear Energy*, 2021. 150. https://www.sciencedirect.com/science/article/pii/S0306454920305272

26. Jessee, M.A., W.A. Wieselquist, U. Mertyurek, K.S. Kim, T.M. Evans, S.P. Hamilton, and C. Gentry, "Lattice Physics Calculations Using the Embedded Self-Shielding Method in Polaris, Part I: Methods and Implementation." *Annals of Nuclear Energy*, 2021. 150. https://www.sciencedirect.com/science/article/pii/S0306454920305284

27. Gauld, I.C., "Validation of ORIGEN-S Decay Heat Predictions for LOCA Analysis." PHYSOR-2006: American Nuclear Society's Topical Meeting on Reactor Physics - Advances in Nuclear Analysis and Simulation, Vancouver, BC (Canada). 2006.

28. Gauld I.C., Ilas G., Murphy B.D. and Weber C.F., *Validation of SCALE 5 for Decay Heat Predictions of LWR Spent Fuel*, 2010. NUREG/CR-6972, US Nuclear Regulatory Commission. www.nrc.gov/reading-rm/doc-collections/nuregs/contract/cr6972/

29. Ilas, G. and I.C. Gauld, "SCALE Analysis of CLAB Decay Heat Measurements for LWR Spent Fuel Assemblies." *Annals of Nuclear Energy*, 2008. 35(1): p. 37. https://doi.org/10.1016/j.anucene.2007.05.017

30. Ilas, G., I.C. Gauld, and H. Liljenfeldt, "Validation of ORIGEN for LWR Used Fuel Decay Heat Analysis with SCALE." *Nuclear Engineering and Design*, 2014. 273: p. 58. https://doi.org/10.1016/j.nucengdes.2014.02.026

31. Ilas, G. and H. Liljenfeldt, "Decay Heat Uncertainty for BWR Used Fuel Due to Modeling and Nuclear Data Uncertainties." *Nuclear Engineering and Design*, 2017. 319: p. 176. https://www.sciencedirect.com/science/article/pii/S0029549317302376

32. Sunny, E.E., Ilas, G. "SCALE 6 Analysis of HTR-10 Pebble-Bed Reactor for Initial Critical Configuration." *PHYSOR 2010 International Conference on Reactor Physics*. 2010. Pittsburgh, PA.

33. G. Ilas, D.Ilas, R.P. Kelly, and E.E. Sunny, *Validation of SCALE for High Temperature Gas-Cooled Reactor Analysis*, 2012. NUREG/CR-7107, US Nuclear Regulatory Commission. www.nrc.gov/docs/ML1211/ML12116A124.pdf

34. Ilas, D., "SCALE Code Validation for Prismatic High-Temperature Gas-Cooled Reactors." *Nuclear Technology*, 2013. 183(3): p. 379. https://doi.org/10.13182/NT13-A19426

35. Bostelmann, F., C. Celik, M.L. Williams, R.J. Ellis, G. Ilas, and W.A. Wieselquist, "SCALE Capabilities for High Temperature Gas-Cooled Reactor Analysis." *Annals of Nuclear Energy*, 2020. 147. https://www.sciencedirect.com/science/article/pii/S0306454920303716

36. Godfrey, A.T., J.C. Gehin, K.B. Bekar, and C. Celik, "Simulation of Watts Bar Initial Startup Tests with Continuous Energy Monte Carlo Methods," 2015. *Proc. of the International Conference on Physics of Reactors* (PHYSOR2014), Kyoto, Japan http://inis.iaea.org/search/search.aspx?orig_q=RN:47042902

37. Godfrey, A.T., B.S. Collins, K.S. Kim, R. Montgomery, J.J. Powers, R.K. Salko, S.G. Stimpson, W.A. Wieselquist, K.T. Clarno, J.C. Gehin, S. Palmtag, R. Montgomery, D. Jabaay, B. Kochunas, T. Downar, N.A. Capps, and J. Secker, "VERA Benchmarking Results for Watts Bar Nuclear Plant Unit 1 Cycles 1–12, 2016. *Proc. PHYSOR-2016*, Sun Valley, ID.

38. Broadhead, B.L., M.D. DeHart, J.C. Ryman, J.S. Tang, and C.V. Parks, *Investigation of Nuclide Importance to Functional Requirements Related to TRANSPort and Long-Term Storage of LWR Spent Fuel*, 1995. ORNL/TM-12742, Oak Ridge National Laboratory https://www.osti.gov/servlets/purl/95570

39. Gauld, I.C. and J.C. Ryman, *Nuclide Importance to Criticality Safety, Decay Heating, and Source Terms Related to Transport and Interim Storage of High-Burnup LWR Fuel, 2000*. NUREG/CR-6700 US Nuclear Regulatory Commission. https://www.osti.gov/servlets/purl/799527

40. *Spent Nuclear Fuel Assay Data for Isotopic Validation (State-of-the-Art Report)*, 2011. Nuclear Energy Agency https://www.oecd-nea.org/science/wpncs/ADSNF/SOAR_final.pdf

41. Ilas, G. and I.C. Gauld, "Analysis of Isotopic Assay Data from the MALIBU Program," 2008. PHYSOR-2008 International Conference on Reactor Physics: Nuclear Power A Sustainable Resource, Interlaken, Switzerland.

42. DeHart, M.D. and S.M. Bowman, "Reactor Physics Methods and Analysis Capabilities in SCALE." *Nuclear Technology*, 2011. 174(2): p. 196. https://doi.org/10.13182/NT174-196

43. Gauld, I.C., G. Radulescu, G. Ilas, B.D. Murphy, M.L. Williams, and D. Wiarda, Isotopic "Depletion and Decay Methods and Analysis Capabilities in SCALE." *Nuclear Technology*, 2011. 174(2): p. 169. https://doi.org/10.1016/j.anucene.2012.03.012

44. Rearden, B.T., B.R. Betzler, M.A. Jessee, W.J. Marshall, U. Mertyurek, and M.L. Williams, "Accuracy and Runtime Improvements with SCALE 6.2," 2016. *Proc. M&C 2017*, Jeju, South Korea https://www.osti.gov/servlets/purl/1376415

45. Ilas, G., B. Hiscox., "Validation of SCALE 6.2.4 and ENDF/B-VII.1 Data Libraries for Nuclide Inventory Analysis in PWR Used Fuel," 2021. *Transactions of the American Nuclear Society*, 124, p.552-554 (2021). https://www.ans.org/pubs/transactions/article-49653/

46. Ilas, G., J.R. Burns., "SCALE 6.2.4 Validation for Light Water Reactor Decay Heat Analysis." *Nuclear Technology*, 2021. https://doi.org/10.1080/00295450.2021.1935165

47. Ilas, G., H. Liljenfeldt. "Decay Heat Uncertainty for BWR Used Fuel Due to Modeling and Nuclear Data Uncertainties," 2017. SCALE Users' Group Workshop. https://www.ornl.gov/scale/scale/2017-scale-users-group-workshop

48. Akkurt, H. , H. Liljenfeldt, G. Ilas, S. Baker, K. Fuhr, 2020. *Phenomena Identification and Ranking Table (PIRT) for Decay Heat: Review of Current Status and Recommendations for Future Needs*, EPRI Report 3002018440, https://www.epri.com/research/products/000000003002018440

49. Shama, A., D. Rochman, S. Pudollek, S. Caruso, and A. Pautz, "Uncertainty Analyses of Spent Nuclear Fuel Decay Heat Calculations Using SCALE Modules." *Nuclear Engineering and Technology*, 2021. https://www.sciencedirect.com/science/article/pii/S1738573321001558

50. Terry W.K. , L.M. Montierth, S. S. Kim, J. J. Cogliati, and A. M. Ougouag, "Evaluation of the Initial Critical Configuration of the HTR-10 Pebble-Bed Reactor," 2009. I*nternational Handbook of Evaluated Reactor Physics Benchmark Experiments*, Nuclear Energy Agency.

51. Bess J. D., Fujimoto N., "Evaluation of the Start-Up Core Physics Tests at Japan's High Temperature Engineering Test Reactor (Fully-Loaded-Core)," 2010. HTTR-GCR-RESR-001, Revision 1, *International Handbook of Evaluated Reactor Physics Benchmark Experiments*, Nuclear Energy Agency.

52. Mertyurek, U., B.R. Betzler, M.A. Jessee, and S.M. Bowman, "SCALE 6.2 Reactor Physics Code Accuracy Assessment for Light Water Reactor Fuel," 2018. *PHYSOR-2018*. https://www.osti.gov/servlets/purl/1559746